Ann. Phys. (Berlin) **529**, No. 7, 1600350 (2017) / DOI 10.1002/andp.201600350

annalen der physik

Review Article

The ergodic side of the many-body localization transition

David J. Luitz[1,*] *and Yevgeny Bar Lev*[2,1,**]

Received 1 November 2016, revised 20 February 2017, accepted 24 March 2017
Published online 16 May 2017

Recent studies point towards nontriviality of the ergodic phase in systems exhibiting many-body localization (MBL), which shows subexponential relaxation of local observables, subdiffusive transport and sublinear spreading of the entanglement entropy. Here we review the dynamical properties of this phase and the available numerically exact and approximate methods for its study. We discuss in which sense this phase could be considered ergodic and present possible phenomenological explanations of its dynamical properties. We close by analyzing to which extent the proposed explanations were verified by numerical studies and present the open questions in this field.

1 Introduction

Boltzmann's ergodic hypothesis — central to classical statistical mechanics — allows to derive most equilibrium results. It states that a trajectory of a system with many degrees of freedom will spend equal times in regions of equal phase-space measure [1]. This implies that the infinite time average of observables is equivalent to their ensemble average. Attempts to generalize this definition of ergodicity to quantum systems had begun with the works of von Neumann [2, 3] and substantial progress was made in the 1980ies both analytically and numerically in pioneering works by Berry, Pechukas, Peres, Feingold, Jensen and Shankar [4–12], culminating in the contributions by Deutsch [13] and Srednicki [14–16]. It was realized early on that not all complex systems are ergodic, as in particular classically or quantum integrable systems are nonergodic almost by definition. These systems are however not generic since integrability and thus nonergodicity is inherently unstable to the addition of generic perturbations [13]. Ergodicity breaking in more generic systems occurs during thermodynamic phase transitions, where a system spontaneously breaks a symmetry when it orders [17]. A novel mechanism of ergodicity breaking in *generic disordered quantum* systems was proposed ten years ago in a seminal work by Basko, Aleiner and Altshuler, a phenomenon now widely known as many-body localization (MBL) [18]. This work established the stability of the nonergodic Anderson insulator to the addition of weak interactions at sufficiently small but *finite* energy densities, and the stability of the (ergodic) metal for sufficiently large energy densities. It therefore predicted the existence of a critical energy density (the so called many-body mobility edge) which demarcates the ergodic and the nonergodic phases. Unlike ergodicity breaking at thermodynamic transitions, this transition relies on the system being completely *isolated* from the environment and has no signatures in *static* thermodynamic quantities. The existence of a nonergodic phase was recently rigorously proved for one-dimensional random spin chains under a few physically reasonable assumptions [19, 20]. Since MBL requires isolation from the environment, its realization in conventional condensed matter systems is challenging [21, 22]. However signatures of MBL were observed in ultracold atomic gases on optical lattices both in one-dimensional [23–25] and two-dimensional systems [26].

Most works on MBL concentrated on the study of the nonergodic phase, paying little attention to the ergodic phase [27–29]. The reason for this "injustice" is that following the work of Basko, Aleiner and Altshuler it was largely accepted that the ergodic phase in systems exhibiting the MBL transition is a trivial metal, namely it has a finite dc conductivity [18]. Systems with unbounded energy density, which were considered in this work, are essentially classical at sufficiently high energy densities and therefore have a finite dc conductivity as can be shown using a self-consistency argument [18]. For systems with bounded energy density this is not the case

* Corresponding author: E-mail: dluitz@illinois.edu
** E-mail: yb2296@columbia.edu
[1] Department of Physics and Institute for Condensed Matter Theory, University of Illinois at Urbana-Champaign, Urbana, Illinois 61801, USA
[2] Department of Chemistry, Columbia University, 3000 Broadway, New York, New York 10027, USA

since even at infinite temperature there are examples of systems which are far from being classical [30]. First evidence of the nontriviality of the ergodic phase for systems with bounded energy density was obtained by one of us [31]. Using a combination of nonequilibrium perturbation technique and exact diagonalization (see Section 5 for a brief description of these methods) a surprisingly slow relaxation of the density autocorrelation function was observed on the ergodic side of the MBL transition which was attributed to the existence of an intermediate phase with impeded transport due to localized inclusions [31]. In a subsequent work, an extensive study of spin transport in a large portion of the parameter phase space was performed using exact diagonalization (ED) and the time-dependent density matrix renormalization group (tDMRG) [32]. This study showed that most of the ergodic phase is subdiffusive up to simulated times and argued that the dc conductivity must vanish if subdiffusion persists asymptotically in time. Similar results were obtained in the study of ac conductivity, where also a phenomenological explanation of the observed subdiffusion was suggested [33].

In this review we concentrate on the ergodic phase and refer the reader who is interested in the nonergodic phase or the MBL transition to Refs. [27–29] as also to more recent reviews to appear in the current issue [34–37]. We limit the discussion to models with quenched disorder and refer the reader interested in systems with quasiperiodic potentials to Ref. [38] for a review. The structure of the review is the following: in Sec. 2 we present the models which will be used throughout the review, in Sec. 3.3 we survey the properties of the ergodic phase and discuss in which sense this phase is ergodic. In Sec. 4 we present the phenomenological theory of the ergodic phase. Finally, we close the review by surveying the available numerical techniques in Sec. 5 and discuss open questions in Sec. 6.

2 Models

In this section we will introduce the models which will be used throughout the rest of the review. Currently the most studied model in the context of many-body localization is the XXZ model,

$$\hat{H} = \frac{J_{xy}}{2}\sum_{i=1}^{L-1}\left(\hat{S}_i^+\hat{S}_{i+1}^- + \hat{S}_i^-\hat{S}_{i+1}^+\right) + J_z\sum_{i=1}^{L-1}\hat{S}_i^z\hat{S}_{i+1}^z + \sum_{i=1}^{L}h_i\hat{S}_i^z, \tag{1}$$

were $\hat{S}_i^z$, is the $z-$projection of the spin-1/2 operator, $\hat{S}_i^\pm$, are the corresponding lowering and raising operators, J_{xy} and J_z are inter-spin couplings and h_i are random magnetic fields taken to be uniformly distributed in the interval $h_i \in [-W, W]$. This model conserves the $z-$projection of the total spin. Using the Jordan-Wigner transformation [39],

$$\begin{aligned}\hat{S}_i^z &\to \hat{n}_i - \frac{1}{2} \\ \hat{S}_i^+ &\to (-1)^{\sum_{k=1}^{i-1} n_k}\,\hat{c}_i^\dagger \\ \hat{S}_i^- &\to (-1)^{\sum_{k=1}^{i-1} n_k}\,\hat{c}_i,\end{aligned} \tag{2}$$

it can be exactly mapped to a model of spinless electrons,

$$\hat{H} = -t\sum_{i=1}^{L-1}\left(\hat{c}_i^\dagger\hat{c}_{i+1} + \hat{c}_{i+1}^\dagger\hat{c}_i\right) + U\sum_{i=1}^{L-1}\left(\hat{n}_i - \frac{1}{2}\right)\left(\hat{n}_{i+1} - \frac{1}{2}\right) + \sum_{i=1}^{L}h_i\hat{n}_i, \tag{3}$$

where $\hat{c}_i^\dagger$ creates a spinless fermion on site i and $\hat{n}_i = \hat{c}_i^\dagger\hat{c}_i$ is the fermion density. We dropped a constant term and set $t \equiv -J_{xy}/2$ and $U \equiv J_z$ to have a more conventional notation for fermions. The conservation of $z-$projection of the total spin translates to the conservation of the total charge in the fermionic model. In most studies either the hopping t, or the in plane coupling, J_{xy}, are set to be one. We will pursue the latter convention here. Thus, unless otherwise specified, all times are measured in units of J_{xy}^{-1}. For $J_z = 1$ ($U/t = 2$) both models have an ergodic to nonergodic transition for a disorder strength of $W = 3.7 \pm 0.1$ [40]. Since in this review we focus on the ergodic side of the transition, we mostly consider $W \leq 3.7$ here.

Another model which we will discuss is the Anderson-Hubbard model,

$$\hat{H} = -t\sum_{\sigma,i=1}^{L-1}\left(\hat{c}_{i\sigma}^\dagger\hat{c}_{i+1,\sigma} + \hat{c}_{i+1,\sigma}^\dagger\hat{c}_{i\sigma}\right) + U\sum_{i=1}^{L}\left(\hat{n}_{i\uparrow} - \frac{1}{2}\right)\left(\hat{n}_{i\downarrow} - \frac{1}{2}\right) + \sum_{i=1}^{L}h_{i\sigma}\hat{n}_{i\sigma}, \tag{4}$$

where $\hat{c}_{i\sigma}^\dagger$ creates a spinful fermion on site i and $\hat{n}_{i\sigma} = \hat{c}_{i\sigma}^\dagger\hat{c}_{i\sigma}$ is the corresponding density. The disorder potential $h_{i\sigma}$ is taken to be different for the two species in order to explicitly break $SU(2)$ symmetries in the charge and the spin sectors thus avoiding possible complications [41, 42]. While this model naturally appears in cold atoms experiments it is less popular than the XXZ

model, mostly because it has a larger local Hilbert space dimension, which makes it more challenging for numerical study.

Further models, which display an ergodic to nonergodic transition, are periodically driven systems. In these models, also knowns as Floquet-MBL models, the transition can be tuned by the frequency or the amplitude of the drive. We have decided to exclude these systems from our review due to scarcity of numerical results on their dynamics in the ergodic phase. A reader interested in these topics is referred to the recent literature [43–51] and the review Ref. [37].

3 Properties of the Ergodic Phase

In this section we survey the numerical results on the properties of the ergodic phase. Since the XXZ model (1) is equivalent to the spinless fermion model (3), in order to avoid repetition we use the spin language in the rest of the review. Readers who prefer to think in terms of fermions are referred to the mapping (2). To minimize the notational overhead we assume that all the considered quantities are *implicitly averaged over disorder realizations*, and therefore are translationally invariant on average. In this section we will also uniformly use periodic boundary conditions and average over the volume of the system, which we believe enhances readability and allows to operate with more physically transparent formulas. Readers who are interested in the technicalities and precise implementations are referred to Section 5 or to the original works.

3.1 Three flavors of ergodicity

We have postponed the precise definition of ergodicity which we use in this review to this subsection due to the involved subtleties. While the definition for classical systems, via Boltzmann's ergodic hypothesis, presented in the beginning of the introduction is very precise, currently, there is no commonly accepted definition of ergodicity of quantum systems [10, 52]. Some of the reasons for this are that some concepts from classical physics like: microstates, phase-space and chaos cannot be immediately carried over to quantum systems. Here, we discuss three different notions of ergodicity in quantum systems based on (i) the statistics of eigenvalues, (ii) the statistics of eigenvectors and (iii) the validity of the eigenstate thermalization hypothesis.

3.1.1 Eigenvalue statistics

For quantum systems which are chaotic in their classical limit it was conjectured by Bohigas, Giannoni and Schmit that the eigenvalue statistics follow the statistics of an ensemble of random matrices, which depends on the symmetries of the Hamiltonian [53]. Using semi-classical field theory this conjecture was later justified [54]. For systems without a proper classical limit, such as fermionic lattice models or spin systems, a direct connection between eigenvalue statistics and ergodicity is still lacking. Nevertheless, it was empirically shown that many generic quantum systems do follow the eigenvalue statistics of random matrices [55, 56]. To study the eigenvalue statistics, the eigenvalues of the systems are calculated and ordered ascendantly, then, traditionally, "unfolding" of the spectrum is performed, which eliminates the dependence of the statistics on the density of states. The distribution of the unfolded spacings is then obtained and compared to the corresponding random matrix distribution (Wigner-Dyson (WD) distribution). A system is assumed to be ergodic if the distribution of its eigenvalue spacing follows the WD distribution. The distribution of eigenvalue spacings in disordered (Coulomb) interacting systems was studied a decade *before* MBL was established [57–60]. In these early studies a crossover from a Poisson to a WD distribution was observed. In later studies eigenvalue statistics for disordered spin chains were also studied in the context of quantum chaos [61–63]. In the context of MBL eigenvalue statistics was first considered in Ref. [64] which introduced a useful metric for short-range correlations in the eigenvalues statistics, effectively eliminating the arbitrariness which exists in the unfolding procedure [65]. Instead of unfolding, the eigenvalue spacings $\delta_n = E_{n+1} - E_n$ (where E_n are the ordered eigenvalues) are normalized by their magnitude, $r_n = \min(\delta_n/\delta_{n+1}, \delta_{n+1}/\delta_n)$ [66]. Ergodicity is assumed when the obtained probability distribution of r_n (or the unfolded δ_n) matches the one of the corresponding random matrix ensemble [67]. The fact that the phase, which is the subject of this review, is ergodic in this sense was first established in Ref. [66] and then repeatedly in almost every work on MBL.

The distribution of the eigenvalue spacings can be viewed as a stationary distribution of a Brownian motion in a space of Hamiltonians, where at each step a different disorder realization is drawn [68, 69]. In this approach, commonly known as the effective plasma model, unfolded eigenvalues are thought of as particles with an effective two-body interaction which is responsible for the eigenvalue repulsion. By noting that in a second

order expansion in the disordered potential the effective interaction is well described by a power law, Serbyn and Moore derive the corresponding limiting spacings distribution,

$$P(\delta_n) = C_1 \delta_n^{\beta} \exp\left(-C_2 \delta_n^{2-\gamma}\right), \tag{5}$$

where $C_{1,2}$ are constants, $0 \leq \beta \leq 1$ controls the level repulsion and γ controls the tail of the distribution [70]. This distribution interpolates between the Poisson distribution $\gamma = 1$, $\beta = 0$ and the WD distribution $\gamma = 0$, $\beta = 1$. Motivated by this form Serbyn and Moore numerically obtain γ within the whole ergodic phase, even outside the region of validity of the effective plasma model ($W \gtrsim$). It is argued that while for weak disorder $W \lesssim 2$ the spacings distribution appears to flow to the WD distribution, for stronger disorder close to the MBL transition $2 \lesssim W \lesssim 3.7$ a region with intermediate statistics is found. The corresponding distribution is similar to the critical distributions obtained for Anderson transitions, it has an exponential tail $\gamma = 1$ and a *finite* level repulsion $\beta > 0$ [71]. It is therefore argued that the MBL transition has critical statistics similar to the critical Anderson statistics.[1] The effective model used by Serbyn and Moore was criticized in a follow-up exact diagonalization work [72], which pointed out that the eigenvalue statistics of the ergodic phase does not appear to be scale invariant as the plasma model of Ref. [70] suggests, moreover the critical eigenvalue statistics seems to better agree with a Poisson distribution, similarly to critical statistics of Anderson transition on a Bethe lattice.

3.1.2 Eigenvector statistics, multifractality and the "bad metal"

The first proposal of an intermediate phase sandwiched between the deeply ergodic and nonergodic (MBL) phases appeared almost 20 years ago [73]. This phase, colloquially dubbed by Altshuler a "bad metal" [74], was first defined as a delocalized yet nonergodic phase. The definition of ergodicity and delocalization in this context is however quite different from what we have discussed above, therefore to avoid confusion we will use a typewriter font face to designate this kind of `ergodicity`.

The motivation behind this definition is best understood for the case of a single particle. The moments of the eigenstates of the single particle Hamiltonian $\psi_\alpha(x)$ written in the position basis are given by,

$$I_q^\alpha = \sum_x |\psi_\alpha(x)|^{2q}. \tag{6}$$

Delocalized single-particle eigenstates (for example eigenvectors of a random matrix) scale as $\psi_\alpha(x) \sim V^{-1/2}$ where V is the volume of the system, which yields $I_q^\alpha \propto V^{-(q-1)}$. Localized eigenstates which decay exponentially with distance from some localization center, yield $I_q^\alpha \approx$ const. Since the infinite time average of the density autocorrelation function is given by I_2^α (see derivation in Eq. (24)), a natural definition of a delocalized (localized) state would be a state with $I_2^\alpha \to 0$ ($I_q^\alpha \to$ const) for $V \to \infty$. The participation ratio $1/I_2^\alpha$ quantifies the number of sites that a eigenstate occupies in *real* space. When this number of sites is extensive, the system is defined to be `ergodic`. On the contrary when eigenstates cover a subextensive volume in real space $I_2^\alpha \sim V^{-D_2}$ with $0 < D_2 < 1$, not all sites in real space are "available" and the system is therefore `nonergodic`. The eigenstate will be called multifractal if the generalized dimensions D_q depend on q. It occurs, for example, at the critical point of the Anderson transition, where all the moments I_q^α follow an anomalous scaling $I_q^\alpha \sim V^{-D_q(q-1)}$ [71]. We stress that the sparseness of the eigenstates in real space does *not* imply that a generic initial condition will be locked to a region in space. In fact almost all initial conditions will explore the whole volume of the lattice. The sparseness of the eigenfunctions in real space has implications on the *dynamics* of the wavepackets, which will be subdiffusive with a dynamical exponent which could be related to the generalized dimension D_2 [75, 76].

The many-body problem is equivalent to a single-particle hopping on a complicated graph, where the nodes of the graph represent many-body states weighted by the diagonal part of the Hamiltonian and the hopping rates are given by the offdiagonal part. The apparent simplicity of this view is however misleading, since the disorder (many times taken to sit on the diagonal part) will be highly correlated. The number of return paths on this graph is exponentially small in their length, therefore by neglecting the loops it could be approximately mapped to a Cayley tree [73] (see also review by Imbrie *et al.* [34]). Using this analogy one can carry over the above definition of `ergodicity` to the many-body case by substitution of the volume in real space by the total number of many-body states, $\mathcal{N}$,

$$I_q^\alpha = \sum_n |\langle \alpha | n \rangle|^{2q} \propto \mathcal{N}^{-D_q(q-1)}, \tag{7}$$

[1] We note that the level statistics with $\beta > 0$ and $\gamma = 1$ was called a semi-Poisson statistics in Ref. [70]. To eliminate the confusion with semi-Poisson statistics which was introduced in Ref. [237] and implies $\beta = 1$ and $\gamma = 1$, we have instead used the term "critical statistics."

where $|\alpha\rangle$ are the eigenstates of the Hamiltonian computed in some basis $|n\rangle$. We note in passing that this quantity is closely related to the basis dependent Rényi "participation" entropies of the wave function as considered in [40, 77, 78],

$$S_q^{P,\alpha} = \frac{1}{1-q} \ln I_q^\alpha \propto D_q \ln \mathcal{N}. \tag{8}$$

In the limit of $q \to 1$ it reduces to the Shannon entropy $S_1^{P,\alpha} = -\sum_n |\langle\alpha|n\rangle|^2 \ln |\langle\alpha|n\rangle|^2$, and allows to define D_1 as of $S_1^\alpha / \ln \mathcal{N}$. There are a few problems with this definition of `ergodicity`. First, while the real space basis is a natural choice for the single particle problem there is no obvious choice of the basis $|n\rangle$ in the many-body case. The second and more serious problem is the lack of a direct connection between the spreading of the wavepacket on a complicated graph or tree in the many-body Hilbert space and the dynamics in real space (*cf.* Eq. (23) for one possible connection). In particular, it is not clear whether the sparseness of the eigenfunctions in the many-body space ($D_q < 1$) has implications on the thermalization in *finite* many-body systems, or has a signature in local observables (for a discussion see Ref. [79]).

The existence of a stable delocalized but `nonergodic` phase was tested in numerous numerical studies. Most studies of multifractality are focused on either the Bethe lattice or random-regular graphs. After almost a decade of study, this question is still largely open [80–88], while most extensive numerical studies suggest that this phase disappears in the thermodynamic limit [85, 87]. For physical lattice models this question was considered in a study of a random Josephson array [89] and for the XXZ model [40, 90, 91], with a similar inconclusive outcome. While Ref. [40] suggests that $D_1 = 1$ below the MBL transition, Refs. [89, 91] argue in favor of a stable intermediate phase with $D_2 < 1$. Furthermore, Ref. [90] argues that this phase shrinks to the MBL critical point in the thermodynamic limit. We would like to point out that it is possible that this apparent discrepancy might follow from a different basis used to calculate I_q^α in these works [40, 90, 91].

An attempt to connect the notion of `ergodicity` from eigenvector statistics to ergodicity defined through eigenvalues statistics was performed by Serbyn and Moore in the work described above [70]. By using a specific choice of the basis $|\psi^\beta\rangle \equiv 2\hat{S}_i^z |\beta\rangle$ (where $|\beta\rangle$ are the eigenstates of the Hamiltonian) in (7) one can write,

$$I_q^\alpha = \sum_\beta \left|\langle\alpha|\psi^\beta\rangle\right|^{2q} \propto \mathcal{N}^{-D_q(q-1)}, \tag{9}$$

where the scaling with the size of Hilbert space is taken as an assumption (only I_2^α was considered in Ref. [70]). A similar scaling of the moments, was conjectured in Ref. [92] and was recently numerically verified [90]. Using heuristic arguments, Serbyn and Moore connected the exponent γ in (5), which parametrizes the distribution of the eigenvalue spacing to the generalized dimension $\gamma = 1 - D_2$.[2] This relation was however never verified numerically.

3.1.3 Eigenstate thermalization hypothesis

In this review we utilize yet another definition of ergodicity, which is more similar to the Boltzmann ergodic hypothesis for classical systems [1] as also to ideas by von Neumann [2, 3]. It is commonly known as the *eigenstate thermalization hypothesis* (ETH) and it was mostly developed by Deutsch and Srednicki more than two decades ago [13–16, 93], based on a multitude of theoretical and numerical works in quantum chaos [5–12] (for recent reviews, see [79, 94, 95]). One can show that a sufficient condition for local quantum observables $\hat{O}$ to decay to their microcanonical value (and to stay close to this value for sufficiently long times) is the validity of the ansatz,

$$\left\langle \alpha \left| \hat{O} \right| \beta \right\rangle = \bar{O}(E)\, \delta_{\alpha\beta} + e^{-S(E)/2} f(E, \omega)\, R_{\alpha\beta}, \tag{10}$$

where $|\alpha\rangle$, $|\beta\rangle$ are eigenstates of the Hamiltonian, $S(E)$ is the microcanonical entropy, $\bar{O}(E)$, $f(E, \omega)$ are smooth functions of their arguments with $E \equiv (E_\alpha + E_\beta)/2$ and $\omega = E_\beta - E_\alpha$ and $R_{\alpha\beta}$ are random independent variables with zero mean and a unit variance.

The fact that the ergodic phase is indeed ergodic under this definition was established for the diagonal elements in Refs. [96, 97] and for the offdiagonal elements in Ref. [98]. However it was observed that the shape of the probability distributions of local operators in the eigenbasis of the Hamiltonian according to Eq. (10) depends strongly on the value of the disorder strength for both diagonal and off-diagonal matrix elements. In particular, the distributions are perfectly Gaussian for weak disorder, while for intermediate disorder strength the distribution of $R_{\alpha\beta}$ becomes strongly non-Gaussian even in the thermodynamic limit. Interestingly, even in this case, the ETH ansatz remains valid, although in a generalized

[2] We note that there appears to be a misprint in Ref. [70]. Since for $\gamma = 1, d_2 = 1 - \gamma = 0$, while from the authors' definition of $\mathcal{N} \sum_\alpha \left|\langle\alpha|\psi^\beta\rangle\right|^4 \propto \mathcal{N}^{-d_2}$ one gets that, $I_2 \propto \mathcal{N}^{-1}$, which corresponds to a WD distribution ($\gamma = 0$).

form with a non-Gaussian noise term $R_{\alpha\beta}$. These non-Gaussian probability distributions are accompanied with a slower decrease of the standard deviation of the offdiagonal matrix elements $\langle\alpha\,|\,\hat{O}\,|\,\beta\rangle$ with the size of the system in the low frequency limit ($\omega = E_\alpha - E_\beta$). This modified scaling was connected to the dynamical exponent of the system [98]. The dependence of the $\langle\alpha\,|\,\hat{O}\,|\,\beta\rangle$ matrix elements on ω was also studied in Ref. [90].

3.2 Entanglement structure

The ETH ansatz is commonly assumed to hold for few-body operators which have a finite support on a small subsystem of the total isolated system. This implies that even when the whole system is in an eigenstate $|\alpha\rangle$, a sufficiently small subsystem A is thermalized by the rest of the system. Clearly, thermalization requires that the entropy of the subsystem, *i.e.* the von Neumann entanglement entropy obtained by tracing out degrees of freedom that are not in the subsystem A, *(cf.* also the recent review in Ref. [99])

$$S_A^\alpha = -\mathrm{Tr}\left(\hat{\rho}_A \ln \hat{\rho}_A\right), \quad \text{with} \quad \hat{\rho}_A = \mathrm{Tr}_{\bar{A}}|\alpha\rangle\langle\alpha|$$

has to be extensive in the subsystem size $S_A^\alpha \propto L_A$, which is usually referred to as a volume law scaling. In the MBL phase, on the other hand, this is not true and due to the finite localization length, the entanglement entropy of MBL eigenstates scales as the surface area of the subsystem (which is constant in one dimension). This difference in the entanglement scaling across the MBL transition was first observed by Bauer and Nayak [100] numerically and has subsequently become a popular measure to detect the MBL transition [40, 101–104].

Kjäll *et al.* numerically studied the critical region in which the dominant scaling changes from a volume law to an area law [101]. They discovered that close to the transition the *variance* of the entanglement entropy exhibits a maximum. A careful analysis of the probability distributions of the entanglement entropy showed that close to the transition, a *mixture* of volume-law and area-law states exists [97, 104]. In Ref. [104], it was shown that in periodic, disordered, one dimensional systems the average of the entanglement entropy $\bar{S}_A$ over all possible bipartitions with the same subsystem length is a smooth and concave function of the subsystem length L_A. The derivative $\partial\bar{S}_A/\partial L_A$ was argued to capture the dominant entanglement scaling in the system for single eigenstates, and is close to its maximal value ($\ln 2$ for spin-1/2 chains) in the case of a volume law scaling, and zero in the case of an area law scaling. The probability distribution of $\partial\bar{S}_A/\partial L_A$ close to the MBL transition becomes strongly bimodal *even for single disorder realizations* [104], although the inter-sample variance is observed to be smaller than the sample-to-sample variance [104, 105].

At weaker disorder, the probability distributions of the entanglement entropy and its slope are sharply peaked at a large, volume law value, with exponentially suppressed tails at lower entanglement, which neither affect the mean nor the variance. The analysis of the entanglement structure in Ref. [104] seems to exclude the possibility of critical eigenvectors which have a volume law scaling with a suppressed prefactor [106]. Such a sub-thermal volume law scaling holds only for the disorder averaged entanglement entropy and is caused by the disorder average over a sharply peaked bimodal distribution. This average corresponds to a part of the distribution with exponentially low weight and is therefore physically meaningless.

The study of the spatial entanglement structure is especially interesting in light of the rare Griffiths regions picture, which was proposed to explain the observed subdiffusion (see Sec. 4). In Ref. [97], the entanglement entropy was calculated as a function of the cut position, showing qualitatively that in the ergodic phase some cuts between the two subsystems have much lower entanglement entropies compared to other cuts. Moreover these regions can be identified in any eigenstate of the system. The correlation between eigenstates in the spatial variation of entanglement was also observed in the nearest neighbor concurrence as a local probe of entanglement [107]. In an analysis of the probability distribution of the change of the entanglement entropy $\Delta(\ell) = S(\ell+1) - S(\ell)$ if the subsystem is enlarged by one site it was shown that at intermediate disorder there is an increasing probability (when disorder is increased) of finding $\Delta(\ell) < 0$, which can be seen as indirect evidence for the existence of insulating inclusions in the system [104]. To make progress in this direction, it may prove useful to study more local probes of entanglement, such as the mutual information $I(A, B) = S_A + S_B - S_{A\cup B}$, which was recently proposed as a generic measure to extract the correlation length [108].

3.3 Dynamical properties and transport

In this section we will survey the different results on the dynamical properties of the ergodic phase of systems exhibiting MBL transition. To emphasize the similarity between MBL systems and classical glasses through this

section we will adopt the notation commonly used in the glasses community. At the end of the section we present a summary of the relations between the different dynamical quantities.

3.3.1 Mean-square displacement and ac conductivity

The XXZ model conserves both the total energy and the z–projection of the total spin, which is equivalent to the conservation of the total number of particles in the fermion language. For this model one can therefore study either the transport of spin or energy. Following the work of Basko, Aleiner and Altshuler [18] and first numerical studies of the dc conductivity it was largely believed that the ergodic phase is a metal [109–111], namely that it has a finite dc conductivity (similarly to a normal liquids in structural glasses). First evidence of the surprisingly slow relaxation of local observables deep in the ergodic phase was obtained using a self-consistent second Born approximation [31]. A more extensive exploration of transport in the ergodic phase using numerically exact methods was performed in Ref. [32]. In this work the spin-spin correlation function

$$G_r(t) = \mathrm{Re}\,\frac{1}{L}\sum_i \mathrm{Tr}\left[\hat{\rho}_0\,\hat{S}^z_{i+r}(t)\,\hat{S}^z_i(0)\right] \tag{11}$$

was calculated, where $\hat{\rho}_0$ is the density operator of the initial state of the system which is typically taken to be proportional to the identity operator (infinite temperature). This correlation function is analogous to the van Hove correlation function in structural glasses [112], and intuitively describes the evolution of a spin excitation created at time $t = 0$. To assess transport properties one can evaluate the analog of the classical mean-square displacement,

$$x^2(t) = \sum_r r^2 G_r(t)\,, \tag{12}$$

which for diffusive systems should asymptotically scale linearly with time, $x^2 \sim t$. It was found that even for the smallest studied disorder strength ($W \approx 1$) and through most of the ergodic phase transport is subdiffusive,

$$x^2(t) \sim t^{2/z} \qquad \text{for} \qquad t < t_*(J_z, W)\,, \tag{13}$$

with a dynamical exponent, $z(J_z, W) \geq 2$ which depends on the parameters of the system. The simulation time $t_* \approx L^z$ was chosen such that finite-size effects were eliminated up to a predefined precision [32]. This time scale could be considered as a generalized Thouless time, namely the time it takes to transport a particle across the system [72, 90, 98, 113]. An analogous calculation was performed using the self-consistent second Born approximation for a *two-dimensional* Anderson-Hubbard model (4), yielding similar results [114]. The evaluation of (11) and (13) is valid for any initial state and therefore does *not* require the system to be within the linear response regime. However for a thermal initial state $\hat{\rho}_0$ it is directly related to the frequency dependent diffusion coefficient calculated from linear response theory [115] (for a derivation of this relation for quantum systems see Appendix A),

$$D(\omega) = -\omega^2 \int_0^\infty \mathrm{d}t\, \mathrm{e}^{\mathrm{i}\omega t} x^2(t)\,, \tag{14}$$

which is proportional to the ac conductivity,

$$\sigma(\omega) \propto \omega^2 \int_{-\infty}^{\infty} \mathrm{d}t\, \mathrm{e}^{\mathrm{i}\omega t} |t|^{2/z} \propto |\omega|^{1-2/z}. \tag{15}$$

The dependence of the ac conductivity on the frequency was numerically calculated in Refs. [33, 116]. We note in passing that for infinite temperatures what is actually computed is $D(\omega) \sim T\sigma(\omega)$ since $\sigma(\omega)$ vanishes in this limit. At the MBL transition the dynamical exponent is expected to diverge, $z \to \infty$, and therefore the critical ac conductivity is $\sigma(\omega) \propto \omega$ [116]. The ac conductivity was the first dynamical quantity which was studied in the context of MBL. Within the linear response theory its real part is given by the Kubo formula [117],

$$\mathrm{Re}\,\sigma(\omega) = \frac{1}{\omega L}\tanh\left(\frac{1}{2}\beta\omega\right)\int_{-\infty}^{\infty} \mathrm{d}t\, e^{i\omega t}\mathrm{Re}\left\langle \hat{J}(t)\,\hat{J}(0)\right\rangle_\beta\,, \tag{16}$$

where $\beta = 1/T$, and we set the Boltzmann constant to be one, $\langle . \rangle_\beta$ is the thermal expectation value and $\hat{J}$ is the total current density operator,

$$\hat{J} = i\frac{J_{xy}}{2}\sum_n \left(\hat{S}^+_n \hat{S}^-_{n+1} - \hat{S}^+_{n+1}\hat{S}^-_n\right). \tag{17}$$

The use of the Kubo formula above assumes the validity of linear response theory. While the validity of (16) within the ergodic phase was not directly tested, the response of the system for sufficiently small driving fields was shown to be linear [118, 119], as also the heating of the system [120].

The first results on spin and heat ac conductivities were obtained using exact diagonalization (ED) [109]. In this work it was argued that,

$$\sigma(\omega) \backsimeq \sigma_{dc}(J_z, W) + A|\omega| \tag{18}$$

(and similarly for the heat conductivity) with $\sigma_{\rm dc} > 0$ for most J_z and W. The putative delocalization of the MBL phase was later challenged in Ref. [110] and then also in Ref. [111]. Recent large scale ED studies, with systems as large as $L = 28$, confirmed a *linear* scaling with frequency and *a finite* dc conductivity in the *ergodic* phase [121–123], in contrast to the finding of a sublinear scaling (15) and *zero* dc conductivity in the same region of the phase diagram as argued in Refs. [33, 116]. These contradicting results highlight the difficulty of extracting the low frequency behavior from the Kubo formula (16); a difficulty, which was pointed out already by Thouless and Kirkpatrick [124] and more recently by Berkelbach and Reichman [110]. The evaluation of the ac conductivity for any *finite* system requires a broadening of the many-body levels with an artificial width η, which could be attributed to either a residual coupling to the environment or to the timescale over which the conductivity is measured [121]. This coupling results in $\sigma_{dc}(\eta) > 0$ for any finite system. In order to eliminate the dependence on η it is crucial to take the thermodynamic limit $L \to \infty$ before taking $\eta \to 0^+$ [124, 125]. For systems *known* to be metallic ($\sigma_{dc} > 0$), this apparently formidable task is actually feasible, since even for finite systems $\sigma(\omega)$ is almost independent of η, as long as $\eta > \Delta$ (where Δ is the mean level spacing) [124]. This is however *not* the case when it is not known *a priori* if $\sigma_{dc} > 0$, and the way the extrapolation to the thermodynamic limit is performed is extremely important. The main technical difference between Refs. [109, 111, 121–123] and Refs. [33, 116] is the functional form which was used to fit the ac conductivity. While the former works assume a *finite* dc conductivity and the form (18), the later assume that the dc conductivity *vanishes* and the form (15). An attempt to circumvent the inherent finite size constraint of ED studies was performed in Ref. [126], where a continued fraction expansion of dynamical correlations using a variational extrapolation of recurrents was developed. This allowed the authors of Ref. [126] to work essentially at the infinite system limit. The results of this work are consistent with a vanishing dc conductivity and the functional dependence (15).

3.3.2 Autocorrelation function and the Edwards-Anderson parameter

A different way of examining dynamical properties is the calculation of the local autocorrelation function, which is a special case of zero displacement ($r = 0$) in (11),

$$G_0(t) = \frac{1}{L}\mathrm{Re}\sum_{i=1}^{L}\mathrm{Tr}\,\hat{\rho}_0\,\hat{S}_i^z(t)\,\hat{S}_i^z(0)\,. \tag{19}$$

Its infinite time average for thermal initial states, $\hat{\rho}_0 = \exp[-\beta\hat{H}]/Z$ is given by,

$$\lim_{T\to\infty}\int_0^T G_0(\bar{t})\,\mathrm{d}\bar{t} = \frac{1}{L}\sum_i\sum_\alpha e^{-\beta E_\alpha}\left|\langle\alpha\left|\hat{S}_i^z\right|\alpha\rangle\right|^2 = q_{\rm EA}, \tag{20}$$

where $|\alpha\rangle$ and E_α are the eigenvectors and eigenvalues of the Hamiltonian and $q_{\rm EA}$ is the Edwards-Anderson (EA) parameter [127]. Similarly to the situation for spin-glasses the EA parameter is zero in the ergodic phase and nonzero in the nonergodic MBL phase, and could be used as an order parameter of the MBL transition[3] [101, 128–131]. While there is no direct connection between the decay of the autocorrelation function and transport, many times the following relation between the autocorrelation function and the mean-square displacement is assumed to hold (see derivation for subdiffusive classical systems in Sec. 4),

$$G_0(t) \propto \frac{1}{\sqrt{x^2(t)}} = t^{-1/z}, \tag{21}$$

which relies on a scaling hypothesis, and allows to relate between the exponents of the ac conductivity (15) and the autocorrelation function (21) [132]. This relation was also derived in Refs. [33, 116]. The spectral density can be evaluated by taking the Fourier transform of the autocorrelation function,

$$A(\omega) \equiv \int \mathrm{d}t\,\mathrm{e}^{\mathrm{i}\omega t}G_0(t) \propto |\omega|^{-(1-1/z)}\,, \tag{22}$$

which diverges at small frequency [133]. While the autocorrelation function was already considered in Refs. [110, 134], the surprisingly slow relaxation deep in the ergodic phase was noted in Ref. [31], and was attributed to the possibility of an intermediate phase. In fact, a *direct* study of the functional dependence of the dynamical exponent extracted from the autocorrelation function (21) was only performed quite recently [33, 98].

3.3.3 Survival or return probability

For an initial state which is a projector on an eigenstate, $\hat{\rho}_0 = |\alpha\rangle\langle\alpha|$ the autocorrelation function is closely related to the survival probability,

$$C(t) = \left|\langle\alpha\left|\delta\hat{S}_i^z(t)\,\delta\hat{S}_i^z(0)\right|\alpha\rangle\right|^2 = \left|\left\langle\psi_\alpha\left|\mathrm{e}^{-\mathrm{i}\hat{H}t}\right|\psi_\alpha\right\rangle\right|^2, \tag{23}$$

[3] For systems with no (or broken) spin reflection symmetry.

where we have defined, $|\psi_\alpha\rangle \equiv \delta\hat{S}_i^z|\alpha\rangle$, and $\delta\hat{S}_i^z = \hat{S}_i^z - \langle\alpha|\hat{S}_i^z|\alpha\rangle$, to set the infinite time average of $\langle\alpha|\delta\hat{S}_i^z(t)\delta\hat{S}_i^z(0)|\alpha\rangle$ to zero. The decay of the survival probability therefore corresponds to the decay of the *fluctuations* of the autocorrelation function. The infinite time average of the survival probability is given by,

$$I_2 \equiv \lim_{T\to\infty}\frac{1}{T}\int_0^T \mathrm{d}t\left|\sum_\beta |C_{\alpha\beta}|^2 \mathrm{e}^{-\mathrm{i}E_\beta t}\right|^2 = \sum_\beta |C_{\alpha\beta}|^4, \quad (24)$$

where we defined $C_{\alpha\beta} = \langle\alpha|\delta\hat{S}_i^z|\beta\rangle$ and I_2 is the inverse participation ratio. The inverse participation ratio scales as $I_2 \propto \mathcal{N}^{-\tilde{D}_2}$, where $\mathcal{N}$ is the Hilbert space dimension and $\tilde{D}_2$ is a generalized dimension. For delocalized systems (even non-interacting) $\tilde{D}_2 > 0$ and $I_2 \to 0$ in the limit $L\to\infty$, while for localized systems, $\tilde{D}_2 = 0$ and $I_2 \to$ const. There is no direct connection between the decay of the survival probability in many-body systems and transport, yet a power law relaxation was obtained,[4]

$$C(t) \sim t^{-\tilde{D}_2}, \quad (25)$$

with disorder dependent exponent, $0 \le \tilde{D}_2 \le 1$, which is just the generalized dimension defined above [91, 135].

3.3.4 Dynamical structure factor and the imbalance

Instead of studying the decay of local excitations one can also consider the relaxation of collective (spin-wave like) excitations,

$$F(q,t) = \mathrm{Re\,Tr}\left[\hat{\rho}_0\hat{S}_q^z(t)\,\hat{S}_{-q}^z(0)\right], \quad (26)$$

where $\hat{S}_q^z(t) = \sum_n \hat{S}_n^z(t)\exp[iqn]/\sqrt{L}$, and $F(q,t)$ is the analog of the coherent intermediate scattering function in structural glasses [112]. It is simply related to the van Hove correlation function (11) calculated in Refs. [32, 114],

$$F(q,t) = \sum_r G(r,t)\,\mathrm{e}^{-\mathrm{i}qt}, \quad (27)$$

and was directly studied in the context of MBL in Ref. [136]. For diffusive systems this quantity relaxes exponentially, $F(q,t) \sim \exp[-Dq^2t]$, while for supercooled liquids the relaxation is characterized by a Kohlrausch-Williams-Watts (KWW) law, $F(q,t) \sim \exp[-At^\beta]$, and is also known as the $\beta-$relaxation [112]. Taking a Fourier transform of $F(q,t)$ with respect to time gives the dynamical structure factor $S(q,\omega)$ which was recently numerically studied in Ref. [123].

Due to the destructive nature of measurements in cold atoms experiments it is hard to measure two-time correlation functions, however for $q=\pi$ and a Néel state initial condition Eq. (26) reduces to a one time-quantity, dubbed the imbalance,

$$I(t) = \sum_{n=1}^{L}(-1)^n\langle\hat{S}_n^z(t)\rangle, \quad (28)$$

which was successfully measured in a cold atoms experiment [23]. An extensive ED study of the decay of the imbalance (generalized to random product states) was performed by one of us in Ref. [137], where it was found that for systems up to $L \le 28$ the imbalance decays as a power-law superimposed on decaying oscillations,

$$I(t) \sim t^{-\zeta(W)}, \quad (29)$$

moreover the dynamical exponent is subdiffusive, $\zeta(W) < 1/2$ for disorder strengths $W > 0.5$ and vanishes at the MBL transition. The exponent $\zeta(W)$ is related to the dynamical exponent as $\zeta(W) = 1/z$ [98][5].

3.3.5 Entanglement entropy growth

In Ref. [137] it was also demonstrated that after a local quench the entanglement entropy grows only sublinearly with time,

$$S(t) \sim t^{1/z_{\mathrm{ent}}(W)}, \quad (30)$$

such that $z_{\mathrm{ent}}(W) \ge 1$. Similar results were obtained using a light-cone tDMRG, which allows to obtain bulk transport up to some finite time [138]. This study used a binary disorder distribution which allowed to *exactly* average over *all* disorder realizations by utilizing the ancilla trick [139].

If one assumes that "quasi-particles" become entangled on "first encounter" and cannot disentangle, then it is clear that entanglement has to spread faster than transport of particles, $z_{\mathrm{ent}} < z$ [140]. Indeed, due to the conservation of the total spin, in order to reduce the *total* spin in some interval l, one has to transport a "quasi-particle" through the interval l times. On the other hand,

[4] In Ref. [135] a product state initial condition was used, which is different from the initial condition we have used in our definition (23).

[5] This relation is not surprising since for $q=\pi$ the correlation function (26) is very close in form to the local autocorrelation function. For smaller q it however should not be expected.

by the assumption above, to entangle all the "quasi-particles" in this interval, it is enough to transport a "quasi-particle" through it only once. This implies that the time it takes to induce entanglement in this interval is l times smaller than the transport time, $t_{\mathrm{ent}} = t_{\mathrm{tr}}/l$ or,

$$z_{\mathrm{ent}} = z - 1. \tag{31}$$

This heuristic argument establishing the connection between the dynamical exponents z and z_{ent} was introduced in Refs. [102, 103]. While a microscopic derivation of the dynamical exponent z_{ent} and its connection to the dynamical exponent z is still missing, using a novel diagrammatic technique a related quantity was calculated by Aleiner *et al.* [141]. In this work an equation of motion for the out-of-time order correlator was obtained which is similar to equations of motion customary in the field of combustion. The out-of-time order correlator measures the spread of disturbances [142] and is related to the spread of entanglement [143]. Ref. [141] provides therefore a microscopic justification to the "entanglement on first encounter" conjecture raised by Kim and Huse [140]. For a numerical verification of this conjecture see Ref. [144]. Finally, we note that slow information transport was also observed in a sublinear power law growth of the operator entropy of the time evolution operator [145].

3.3.6 Transport from nonequilibrium stationary states

Another initial condition which is useful for cold atoms experiments is the domain wall initial condition, $|\uparrow\cdots\uparrow\downarrow\cdots\downarrow\rangle$, where one measures the decay of the magnetization imbalance between two halves of the system [26]. While for this initial condition dynamics has not yet been studied in an experiment, it was simulated using tDMRG for systems up to $L = 60$ in Ref. [146]. The transported magnetization across the domain wall is consistent with a power law in accord with the scaling (13), $M(t) \sim t^{1/z}$.[6] The domain wall initial condition and the decay of the longest wavelength excitation were also used in an ED study of energy transport [147]. In this work, using a phenomenological diffusion equation and by extrapolating to the thermodynamic limit, an energy diffusion coefficient was calculated. It was argued that energy diffusion coefficient is nonzero through a large portion of the ergodic phase [147].

In condensed matter systems, where the real time dynamics is fast, and therefore mostly inaccessible, transport is normally assessed by the calculation of a stationary state current after the system has been connected to a constant bias. Normal diffusive metals obey Ohm's law with a stationary current which decreases as L^{-1}. For ballistic metals (with mean-free path larger than the system size) the current does not depend on the size of the system and for (perfect) insulators the current decreases exponentially with system size. More generally a relation between the dynamical exponent and the decay of the current can be established using the following classical consideration [148]: The time it takes for one spin to be transported from one side of the system to the other is given by $t_* = L^z$, (which is the generalized Thouless time defined below Eq. (13)). Since a fixed bias makes an extensive number of spins available for transport, $N \propto L$, the stationary current is given by the ratio,

$$j \propto \frac{L}{t_*} = \frac{1}{L^{z-1}}. \tag{32}$$

A power law dependence of the stationary current on the system size was obtained in an open system tDMRG study of the ergodic phase [119]. A direct comparison to the dynamical exponent was not performed there, but it was found that for $W > 0.5$ spin transport in the system is subdiffusive, while for $W < 0.5$ it appears to be diffusive (see Section 5.1 for a description of the method). On the right panel of Fig. 1 we present the dynamical exponent $1/z$ calculated from equation (32) and using the data of Ref. [119]. To highlight the importance of finite size effects we plot the same data, restricting the system sizes to $L < 100$. For $W < 0.6$ and small system sizes ($L < 100$) the transport appears to be faster than diffusive, while for larger sizes ($L < 400$) the transport slows down, yet remaining slightly faster than diffusive, even for the largest system sizes which were used in Ref. [119]. To estimate the *minimal* system sizes for which the effects of the disorder become important, Žnidarič *et al.* calculate the mean-free path in the system in second order perturbation theory in the weak disorder. This length scales as $l \propto W^{-4/3}$,[7] and for $W < 0.6$ becomes larger $l \gg L$ then the system sizes available in ED, making ED an inappropriate numerical tool for the study of such a small disorder. While the results of Ref. [119] are consistent with asymptotic diffusion for $W < 0.6$, whether for even larger system sizes transport slows down and eventually becomes

[6] The authors actually find that a logarithmic time dependence describes their data better, although algebraic growth fits almost equally well.

[7] We note that this scaling is special for the XXZ model which is integrable in the $W = 0$ limit. For more generic nonintegrable models it is supposed to scale as $l \propto W^{-2}$

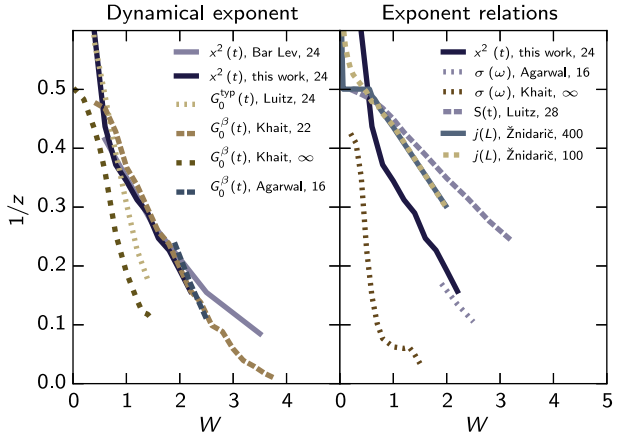

Figure 1 **Left panel:** Dynamical exponent $1/z$. Here we show the finite size results from the Supp. Mat. of Agarwal for $L = 16$ *et al.* [33] and the ED result for $L = 22$ Khait *et al.* [126], obtained from the decay of the infinite temperature correlation function $G_0^{\beta=0}(t)$, as well as the result in the thermodynamic limit using a variational extrapolation of recurrents (VER) by Khait *et al.* [126]. We also show our own result obtained from the same quantity calculated for a (typical) pure state with definite energy, where the functional form of the decay is fitted to include the oscillations [98]. Full lines are the exponents as obtained from the width of the excitation $x^2(t)$ from Ref. [32] (infinite temperature) and calculated for this work for the same typical pure state as mentioned before. **Right panel:** Dynamical exponent estimated through the relations between the exponents from Eq. (33), compared to the best estimate from our calculation of $x^2(t)$ described in the left panel. The exponent extracted from the ac conductivity $\sigma(\omega)$ calculated for a finite system size (16) [33], we also show the thermodynamic limit result obtained from $\sigma(\omega)$ exponent calculated by Khait *et al.* using VER [126]. We include the best estimate of the exponent of the current scaling with system size from Žnidarič *et al.* [119] as well as a our analysis of same data restricted to $L < 100$, and the exponent from the entanglement growth power law from Luitz *et al.* [137].

subdiffusive is still an open question. If this is indeed the case it will suggest that another length scale $\tilde{l}(W, U) > l$ exists in this problem.

3.3.7 Summary

For the convenience of the reader we summarize all the results presented in this subsection,

$$\begin{aligned} x^2(t) &\sim t^{2/z} & G_0(t) \sim I(t) &\sim t^{-1/z} \\ \sigma(\omega) &\sim \omega^{1-2/z} & A(\omega) &\sim \omega^{-(1-1/z)} \\ C(t) &\sim t^{-\tilde{D}_2} & I_2 &\sim \mathcal{N}^{-\tilde{D}_2} \\ j(L) &\sim L^{-(z-1)} & S(t) &\sim t^{1/(z-1)} \end{aligned} \tag{33}$$

where $2 \leq z < \infty$ is the dynamical exponent, the mean-square displacement $x^2(t)$ is defined in (13), the autocorrelation function $G_0(t)$ in (21), the imbalance $I(t)$ in (29), the spectral density $A(\omega)$ in (22), the survival probability $C(t)$ in (23), the inverse-participation ratio I_2 in (24) and $S(t)$ is the entanglement entropy. Here we have considered only disorder averaged quantities. For the discussion of the corresponding typical quantities we refer the reader to Ref. [133].

In Fig. 1 we compare some of the exponent relations which where discussed in this section and are summarized above. We are skipping comparisons of trivial relations which follow from a Fourier transform, such as the comparison between the exponents of $G_0(t)$ and $A(\omega)$. One of the most commonly used and assumed relations is the relation between the decay of the autocorrelation function and the growth of the mean-square displacement $G_0(t) \sim \langle x^2(t) \rangle^{-1/2}$ [see Eq. (21)]. While this equation clearly holds for diffusive transport since the excitation profile $G_r(t)$ is asymptotically Gaussian, there is no reason why it should *a priori* hold for subdiffusive systems where asymptotic excitation profiles can have heavy tails. This relation was indirectly tested in Refs. [33, 126] yielding not a very compelling agreement. In the left panel we perform a direct test of this relation using the dynamical exponent $1/z$ obtained from the decay of the autocorrelation function in three different studies [33, 98, 126], compared to the dynamical exponent computed from the growth of the mean-square displacement [32]. We note that while the results across the studies do agree qualitatively the quantitative discrepancy is pretty large, sometimes as large as 100%. We attribute this discrepancy to the difficulty of fitting power laws to data on a limited time domain and with superimposed oscillations, noting that the growth of the mean-square displacement does not seem susceptible to such problems. Another possible resolution could be that the extracted power-laws are non asymptotic with different measures having different sensitivity to the finite size effects. The relation between the two exponents seems to hold well for $W < 2$ with an increasing discrepancy for stronger disorder, however the difficulty of reliably extracting the autocorrelation exponent precludes from drawing strong conclusions. On the right panel of Fig. 1 we compare the relation between the transport dynamical exponents extracted from the mean-square displacement and the dynamical exponent obtained from the ac conductivity, entanglement entropy and the decay of the

stationary current. Due to relation (40) the ac conductivity exponents and the mean-square exponents have to agree asymptotically, which is indeed what we observe. The exponent extracted from effectively infinite systems is however dramatically different [126]. To the best of our knowledge relation (31) was never explicitly verified for disordered systems. To verify this scaling we plot the transport dynamical exponent $1/z$ and $1/(z_{\text{ent}}+1)$ as obtained in Ref. [137] on the right panel of Fig. 1. It is clear that the relation holds only qualitatively with increasing discrepancy for stronger disorder. Since finite size effects are negligible for strong disorder it appears that the relation between the exponents is more intricate than what is suggested by Eq. (31). Interestingly, while there is a clear violation of the relation (32) the exponent extracted from the current coincides with the exponent extracted from entanglement growth. We note in passing that since entanglement cannot spread faster than particles there is an upper bound of $1/2$ on the value of the $1/z$ exponent extracted from entanglement growth. This means that the agreement for $W<1$ is in some sense trivial, moreover in this regime as was pointed out in the end of Sec. 3.3.6, ED results become increasingly unreliable for such a weak disorder due to severe finite size effects. The apparent violation of relation (32) for strong disorder, where finite size effects are not pronounced has to be better understood.

4 Phenomenological explanations

4.1 Griffiths effects

Anomalous diffusion and subexponential relaxation of autocorrelation functions are often associated with a failure of the central limit theorem and the presence of heavy tailed distributions [149–151]. For example, for classical spin glasses a broad distribution of relaxation times yields a subexponential relaxation of the magnetization and spin autocorrelation functions [152–155], and in the case of Lévy's flights, superdiffusion is a result of a broad distribution of the hopping distances [156]. A broad distribution of relaxation times was also proposed as an explanation for the observed subdiffusion in ergodic one-dimensional systems exhibiting MBL [33]. Microscopically the "fat tail" of the distribution of the relaxation times follows from exponentially rare inclusions which have exponentially long relaxation times and therefore yield non-negligible contributions. Rare region effects on thermodynamical phase transitions were first studied by Griffiths, who noted that quenched disorder can make the free energy non-analytic in a finite temperature interval [157]. The importance of rare spatial regions in quantum phase transitions and for dynamical properties is even more dramatic, therefore rare region effects are overarchingly called Griffiths effects [158]. It was proposed by Agarwal *et al.* that the subdiffusive ergodic phase, which was dubbed the *Griffiths phase*, could be effectively described by a one dimensional random chain governed by the Master equation [33],

$$\frac{\mathrm{d}P_n}{\mathrm{d}t} = W_{n,n-1}\left(P_{n-1}-P_n\right) + W_{n,n+1}\left(P_{n+1}-P_n\right), \tag{34}$$

where P_n is the probability to find a particle on site n and $W_{n,n+1}=W_{n+1,n}>0$ are the corresponding transition rates, which are taken to be independent random variables. This equation had numerous appearances in various contexts. It was first considered by Dyson, more than half a century ago, who calculated the density of states of a random harmonic chain [159]. Replacing P_n by an electric potential on a node n and $W_{n,n+1}$ by random conductances this model is equivalent to a random resistor model, which was used in the hopping conductivity literature [160, 161]. It was also used as a phenomenological model to describe slow relaxation in spin glasses [152–155]. The properties of this model for various distributions of W_n were extensively studied in the 80s by Alexander [132]. It was established that the most important property of the distribution $p(W)$ is whether its $\langle W^{-1}\rangle$ moment exists. If this moment is finite[8] the random chain is diffusive with, $P_0 \sim t^{-1/2}$ and $x^2(t)\sim t$. Otherwise, the system is subdiffusive with an anomalous diffusion which depends on the details of the distribution [132]. For a power law distribution $p(W)\sim W^{-\alpha}$, which was also the distribution considered in Ref. [33], it was rigorously derived that the return probability asymptotically scales as [162],

$$P_0(t) \sim t^{-(1-\alpha)/(2-\alpha)} \qquad \text{when} \qquad P_n(t=0)=\delta_{n0}, \tag{35}$$

with a Laplace transform, $\tilde{P}_0(\omega)\sim\omega^{-1/(2-\alpha)}$. To derive the generalized diffusion coefficient one assumes the scaling form [163],

$$\tilde{P}_n(\omega) \approx \tilde{P}_0(\omega)\, F\left(\frac{n}{\xi(\omega)}\right), \qquad \omega\to 0, \tag{36}$$

where $\xi(\omega)$ is some correlation length and $F(0)=1$. Due to the normalization $\sum_n \tilde{P}_n(\omega)=\omega^{-1}$, and

$$\left(\omega\tilde{P}_0(\omega)\right)^{-1} \approx \sum_n F\left(\frac{n}{\xi(\omega)}\right) \approx 2\int_0^\infty \mathrm{d}x F\left(\frac{x}{\xi(\omega)}\right). \tag{37}$$

[8] In the language of the random resistors this means that the average resistance is finite.

Changing the integration variables $x' = x/\xi(\omega)$ gives,

$$\xi^{-1}(\omega) \approx 2\omega \tilde{P}_0(\omega) \int_0^\infty \mathrm{d}x' F(x'). \tag{38}$$

Now using the relation (14), one can write,

$$D(\omega) = \frac{1}{2}\omega^2 \sum_n n^2 \tilde{P}_0(\omega) = \frac{1}{2}\omega^2 \tilde{P}_0(\omega) \sum_n n^2 F\left(\frac{n}{\xi(\omega)}\right). \tag{39}$$

Changing the variables again and using (38) yields,

$$D(\omega) = \frac{D_0}{\omega \tilde{P}_0^2(\omega)} \sim \omega^{\alpha/(2-\alpha)}, \tag{40}$$

where $D_0 = \int_0^\infty \mathrm{d}x'\, x'^2 F(x')/[8(\int_0^\infty \mathrm{d}x' F(x'))^3]$ [163]. Similar relationships between the exponents of the generalized diffusion coefficient (which is proportional to the ac conductivity) and the return probability were obtained and verified numerically for the XXZ model in Refs. [33, 133]. In dimensions higher than one the random hopping model predicts asymptotically diffusive transport, since contrary to the situation in one dimension, links with low transition rates (high barriers) can be avoided [164]. Nevertheless, transport in a two-dimensional disordered Anderson-Hubbard model (4) was studied by one of us in Ref. [114] and found to be subdiffusive for a broad range of parameters and without visible crossover to diffusion at the studied times.

A simplified explanation of Griffiths effects was presented by Gopalakrishnan *et al.* [133]. It assumed that the system is composed of a collection of independently relaxing regions which additively contribute to the decay of the autocorrelation function, an approach familiar from the spin glass community [153]. The autocorrelation function is taken to be,

$$C(t) = \left\langle \mathrm{e}^{-t/\tau} \right\rangle_\tau \equiv \int_0^\infty \mathrm{d}\tau\ p(\tau) \exp[-t/\tau], \tag{41}$$

where $p(\tau)$ is the density of the regions with relaxation time τ. Instead of using an exponential cutoff, in Ref. [133] a sharp cutoff was assumed, namely,

$$C(t) = \int_t^\infty \mathrm{d}\tau\ p(\tau). \tag{42}$$

Moreover it was assumed that the density of regions and their corresponding relaxation rates are,

$$p(l) \sim \mathrm{e}^{-\gamma l^d} \qquad \tau(l) = \mathrm{e}^{\alpha l}, \tag{43}$$

where α and γ are constants, l is the linear dimension of the region and d is the dimension of the system. We note that these assumptions are reasonable only for autocorrelation functions which do *not* decay to zero in the MBL phase, since only for these correlation functions the relaxation time diverges at the transition. An existence of rare *spatial* regions created by rare local realizations of the disordered potential is also implicitly assumed. Therefore (43) is not expected to hold for deterministic potentials such as the Aubry-André model [133]. From (43) one can calculate the corresponding distribution function of the relaxation times is,

$$p(\tau) \sim \frac{1}{\tau} \exp\left[-\frac{\gamma}{\alpha^d} \ln^d(\tau)\right]. \tag{44}$$

For $d = 1$ the distribution of the relaxation times is given by a power law and the integral in Eq. (42) can be evaluated,

$$C(t) \sim t^{-\gamma/\alpha}, \tag{45}$$

which yields subdiffusive relaxation for $\gamma < 2\alpha$, and a superdiffusive relaxation otherwise. For $d \geq 2$ approximating the integral (42) by the largest integrand yields,

$$C(t) \approx \exp\left[-\frac{\gamma}{\alpha^d} \ln^d t\right], \tag{46}$$

which relaxes faster than any power law, yet slower than exponential [133]. The procedure above is somewhat arbitrary since it strongly depends on the assumed distributions (43). While they have a clear physical meaning, a more microscopic justification would be preferable. Another problem with this approach is that it neglects the dependence between the different regions. While this is a reasonable approximation in higher dimensions, for one dimensional systems it overestimates the relaxation rate since neighboring rare regions should suppress the relaxation of their surrounding. For example, naively calculating the typical autocorrelation function,

$$C(t) \sim \exp[-t/\langle\tau\rangle], \tag{47}$$

yields exponential relaxation, since the average relaxation time $\langle\tau\rangle$ is finite even for one-dimensional systems (for $\alpha < \gamma < 2\alpha$). To correct for this discrepancy one has to take into account the dependence between the regions, which was heuristically performed in Ref. [133]. For a more detailed discussion on the Griffiths effects we refer the reader to Ref. [36].

4.2 Phenomenological renormalization group

Several real space phenomenological renormalization group (RG) approaches were developed to study the

universal features of the MBL transition [102, 103, 165] (for a review see Ref. [35]). A real space coarse-graining of the system is performed, accompanied by a subdivision into ergodic and nonergodic regions. The main difference between the approaches is the way in which these regions are identified and combined during the RG steps. The simplified RG scheme presented in Ref. [165] starts from a random sequence of ergodic and nonergodic regions of different lengths according to some initial distribution. The RG step consists then of identifying the shortest region and merging it with the two neighboring regions. The new region will be ergodic or nonergodic according to a majority rule of the three regions. Using these RG rules the critical distribution can be derived as also the limiting distributions of the ergodic and nonergodic phases. Interestingly, this RG procedure points to a fractal nature of the nonergodic inclusions in the ergodic phase.

This procedure can be viewed as a maximally simplified version of the more detailed RG approach proposed in Ref. [102]. In this work the regions were characterized by their many-body level spacing Δ_i and an entanglement rate Γ_i, which is inversely proportional to the time entanglement spreads across the region. In addition, a set of two-region parameters Δ_{ij} and Γ_{ij} is kept, which correspond to the parameters one would obtain if two neighboring regions were merged. The RG step then consists of merging two regions with the fastest (combined) entanglement rate Γ_{ij}, after which the coupling $\Gamma_{k,ij}$ to the neighboring region k is renormalized. If the coupling between the regions is effective, namely $\Gamma_{ij} \gg \Delta_{ij}$ and $\Gamma_{jk} \gg \Delta_{jk}$ the rates are renormalized according to (a) $\Gamma_{ij;k}^{-1} = \Gamma_{ij}^{-1} + \Gamma_{jk}^{-1} - \Gamma_j^{-1}$, removing double counting of the transversal time of region j. On the other hand, if the coupling is ineffective, the new entanglement rate is obtained from second order perturbation theory via (b) $\Gamma_{ij;k} = \Gamma_{ij}\Gamma_{jk}/\Gamma_j$. For the case when only one of the links is effective there is some arbitrariness in the choice of the rules. If the effective link is between two ergodic regions the rule (a) is used and when the effective coupling is between an ergodic and nonergodic region rule (b) is used. While this RG flow does not permit to directly obtain the entanglement entropy between blocks, it was estimated from the lifetime of product states $1/\Gamma_{ij}$ and the number of accessible states at a given energy $1/\Delta_{ij}$, capturing correctly the transition from a volume law scaling in the ergodic phase to an area law scaling in the nonergodic phase and accompanied by a broad distribution of the entanglement entropy close to the critical point. Transport properties were studied by considering the scaling of the typical transport time l_i/Γ_i with the length of the region l_i. It was found that transport in the ergodic phase in the vicinity of the critical point is subdiffusive with a dynamical exponent smaller then 1/2, while the entanglement growth is sublinear in time.

In Ref. [103] a similar real space RG method was proposed. Unlike the procedures discussed above, in this approach only resonant regions are combined, and the nonresonant regions are left intact. This removes the arbitrariness in RG rules when an ergodic and nonergodic regions have to be combined. Each region has a length l_i and a bandwidth Λ_i, and all the regions are coupled using a coupling strength $\Gamma_{i,j}$ which exponentially decreases with the distance between the regions. After two regions i and j of length l_i (l_j) are merged, the coupling Γ_{ij}, the bandwidth $\Lambda_{ij} = \Lambda_i + \Lambda_j + \Gamma_{ij}$ and the level spacing $\delta_{ij} = \Lambda_{ij}/(2^{l_i+l_j} - 1)$ are renormalized. The coupling to other regions $\Gamma_{ij;k}$ has to be updated too. This is the central step of the renormalization procedure and involves analyzing all possible processes coupling the regions i, j and k. It depends on the energy mismatch δE_{ik} of the individually merged regions i, k or j, k, which is defined as the minimal energy difference in the spectrum of the merged regions. If $\Gamma_{ik} \ll \delta E_{ik}$, then the renormalized coupling can be computed in second order perturbation theory as $\Gamma_{ij;k} = \Gamma_{ik}\Gamma_{ij}/\delta E_{ik}$, otherwise all three regions are strongly coupled and the coupling is given by the addition of the two transport times $\Gamma_{ij;k}^{-1} = \Gamma_{ki}^{-1} + \Gamma_{ij}^{-1}$. Out of all possible processes the largest coupling is retained. Iterating this procedure until all resonant regions are exhausted generates the largest resonant "backbone" in the system. If this backbone percolates across the entire system the system will be ergodic, and nonergodic otherwise.

Potter *et al.* [103] identify subdiffusive transport in the ergodic phase from a broad power law distribution $p(\tau_{ij}) \propto \tau_{ij}^{-\alpha}$ of the transport time scales $\tau_{ij} = 1/\Gamma_{ij}$ with a divergent mean ($1 < \alpha < 2$). The authors argue that transport can be viewed as a random walk (with broadly distributed hopping rates) on the resonant backbone which yields a dynamical exponent of transport of $z = \alpha/(\alpha - 1)$. In contrast to transport, entanglement is not a conserved quantity and spreads deterministically across the chain, thus leading to a different dynamical exponent $z_{\text{ent}} = 1/(\alpha - 1) = z - 1$.

We emphasize that the RG procedures described above are completely phenomenological and are not derived from any microscopic model. A completely different real space RG method, which *is* microscopically based has been introduced in Refs. [129, 166], generalizing the idea of strong disorder RG approaches for ground state properties [167–170]. We refer the reader to the original works in Refs. [129, 166, 171].

5 Numerical methods

In this section we will describe some of the numerically exact and approximate methods which can be used to study the many-body problem. We note that this methods are not limited to the prototype model we have considered in Sec. 2. Through this section we designate the Hilbert space dimension by $\mathcal{N}$ and note that it scales exponentially with the system size, L, e.g. for spin-$\frac{1}{2}$ systems it grows like $\mathcal{N} = 2^L$.

Table 1 Comparison of numerical methods for time evolution. Here m is the number of Krylov vectors, N_t is the number of time steps, χ is the bond dimension, $\mathcal{N}$ is the Hilbert space dimension and L is the system size.

Time evolution	memory	CPU	L	time
ED	$\mathcal{O}(\mathcal{N}^2)$	$\mathcal{O}(\mathcal{N}^3)$	≈ 18	∞
Krylov	$\mathcal{O}(m\mathcal{N})$	$\mathcal{O}(LN_t\mathcal{N})$	≈ 30	$t_{\max}$
tDMRG	$\mathcal{O}(L\chi^2)$	$\mathcal{O}(LN_t\chi^3)$	> 100	$\approx \mathcal{O}(\ln \chi)$

5.1 Exact methods for nonequilibrium time evolution

5.1.1 Full diagonalization

Studying the properties of strongly correlated quantum systems is a formidable problem and an exact treatment of models is often possible only numerically. In a typical nonequilibrium numerical experiment the system is prepared in some initial state $|\psi_0\rangle$, which is not an eigenstate of the Hamiltonian matrix $\mathsf{H} \in \mathbb{C}^{\mathcal{N}\times\mathcal{N}}$. The propagation of the state in time can be performed by exactly diagonalizing the Hamiltonian $\mathsf{H} = \mathsf{U}\mathsf{D}\mathsf{U}^\dagger$, where the matrix $\mathsf{D} = \mathrm{diag}(E_0, \ldots, E_{\mathcal{N}-1})$ is diagonal and contains the eigenvalues E_n of H while the columns of U correspond to the orthonormal eigenvectors $|n\rangle$ (*cf*. Sec. 5.2 for more details). The solution of the Schrödinger equation for the time dependent wave function is given by $|\psi(t)\rangle = \sum_n \mathrm{e}^{-iE_nt}|n\rangle\langle n|\psi_0\rangle$, where $\langle n|\psi_0\rangle$ are the coefficients of the initial wave function in the eigenbasis of the Hamiltonian. If the initial wavefunction is represented as a vector $\mathsf{x}_0 \in \mathbb{C}^{\mathcal{N}}$ in the computational basis, then the wavefunction at time t is obtained by $\mathsf{x}(t) = \mathsf{U}^\dagger\mathrm{e}^{-\mathrm{i}\mathsf{D}t}\mathsf{U}\mathsf{x}_0$, where the matrix exponential of the diagonal matrix D is trivial. While this method is able to access arbitrarily long times, it is limited by the exponential growth of the Hilbert space with the size of the system. The computational complexity of this method is about $\mathcal{O}(\mathcal{N}^3)$, and the required memory is $\mathcal{O}(\mathcal{N}^2)$, effectively limiting the applicability of the method to lattice sizes of $\lesssim 16$ (if the system has no additional symmetries).

5.1.2 Krylov space time evolution

Nautts and Wyatt realized in 1983 [172] that one can avoid the full diagonalization of the Hamiltonian by using a Krylov space method to calculate the exact time evolution $|\psi(t+\Delta t)\rangle = \mathrm{e}^{-\mathrm{i}\hat{H}\Delta t}|\psi(t)\rangle$. Using the series expansion of the exponential, we obtain

$$\mathrm{e}^{-\mathrm{i}\hat{H}\Delta t}|\psi(t)\rangle = \sum_{k=0}^{\infty}\frac{(-\mathrm{i}\Delta t)^k}{k!}\hat{H}^k|\psi(t)\rangle\,, \tag{48}$$

which for very small Δt may be used directly, but is numerically inherently unstable [173]. To obtain a more stable expansion, it is useful to note that the wave function at time $t+\Delta t$ is well approximated by a vector in the m dimensional Krylov space $\mathcal{K}_m = \mathrm{span}(|\psi(t)\rangle, \hat{H}|\psi(t)\rangle, \hat{H}^2|\psi(t)\rangle, \ldots, \hat{H}^{m-1}|\psi(t)\rangle)$. Based on this observation, an orthonormal basis of the Krylov space $\mathcal{K}_m$ is iteratively generated using the numerically stable Arnoldi algorithm [174] and the Hamiltonian is projected into this subspace after m iterations, yielding [173]

$$\mathrm{e}^{-\mathrm{i}\hat{H}\Delta t}|\psi(t)\rangle \approx \mathsf{V}_\mathsf{m}\mathrm{e}^{-\mathrm{i}\mathsf{V}_\mathsf{m}^\dagger\mathsf{H}\mathsf{V}_\mathsf{m}\Delta t}\mathsf{e}_1. \tag{49}$$

Here the columns of the matrix $\mathsf{V}_\mathsf{m} \in \mathbb{C}^{\mathcal{N}\times m}$ contain the orthonormal basis vectors of the Krylov space $\mathcal{K}_m$, and $\mathsf{e}_1 \in \mathbb{C}^m$ is the first unit vector (which corresponds to $|\psi(t)\rangle$ in the new basis as this is the first column of V_m). Note that the matrix $\mathsf{V}_\mathsf{m}^\dagger\mathsf{H}\mathsf{V}_\mathsf{m} \in \mathbb{C}^{m\times m}$ is an upper Hessenberg matrix of *small* dimension $m \ll \mathcal{N}$, which can be readily exponentiated using standard methods, such as a Padé approximation or a rotation to the eigenbasis. The dimension of the Krylov space m is continuously increased until the wavefunction is converged to the desired precision. This method is very powerful since it exploits the sparseness of the Hamiltonian and does not require its full diagonalization. The memory requirements and the computational complexity of this approach are much more favorable compared to exact diagonalization (see Table 1). This approach has been used to study the nonequilibrium dynamics of spin chains with lengths up to $L = 28$ [50, 137, 147].

5.1.3 tDMRG

An independent approach to obtain the numerically exact time evolution of the wave function after a quench employs a representation of the wave function as a *matrix product state* (MPS). For models for which the Hamiltonian can be decomposed into terms which operate on two adjacent sites, which we will call bond terms, the propagation of the wavefunction in time is quite straightforward. In order to calculate the wavefunction after a time step Δt, the Hamiltonian is decomposed into two terms $\hat{H} = \hat{H}_{\text{even}} + \hat{H}_{\text{odd}}$, where $\hat{H}_{\text{even}}$ and $\hat{H}_{\text{odd}}$ contain even (odd) bond terms. While $\hat{H}_{\text{even}}$ and $\hat{H}_{\text{odd}}$ need not commute, all terms within $\hat{H}_{\text{even}}$ ($\hat{H}_{\text{odd}}$) commute with each other. Therefore a Trotter decomposition of the time evolution operator [*cf.* Eq. (48)] can be used to time evolve the state by Δt. The simplest decomposition leads to an error of Δt^2,

$$\mathrm{e}^{-\mathrm{i}\hat{H}\Delta t} = \mathrm{e}^{-\mathrm{i}\hat{H}_{\text{even}}\Delta t}\mathrm{e}^{-\mathrm{i}\hat{H}_{\text{odd}}\Delta t} + \mathcal{O}\left(\Delta t^2\right), \tag{50}$$

however, higher order decompositions can be used (*cf.* Refs. [175, 176]. Note that as the matrix exponentials on the right hand side of Eq. (50) contain only commuting terms, they can be applied sequentially in one DMRG sweep. During the application of the odd and even bond terms to the MPS, the bond dimension of the MPS is adaptively truncated such that the discarded weight, *i.e.* the sum of the discarded singular values does not exceed a certain threshold. As the number of retained singular values directly limits the maximal entanglement entropy that can be encoded by the MPS, it is clear that the bond dimension of the MPS has to grow exponentially with the entanglement entropy. In the ergodic phase the entanglement entropy after a quench from a product state grows as a power law in time [137], thus leading to a stretched exponential growth of the bond dimension with time and effectively limiting this method to short times. In the MBL phase the situation is more favorable since the entanglement entropy grows logarithmically in time [177–180], leading to only a power law growth of the bond dimension. For details on the method, we refer the reader to the original papers on this adaptive method by Vidal [181, 182] and to a review on DMRG [183].

5.1.4 tDMRG for open systems

The study of transport properties can be conveniently performed by opening the system and attaching it to two (or more) leads with a different chemical potential. For Markovian leads and under additional approximations the evolution of the density matrix of the system $\hat{\rho}$ can be described using the Lindblad equation [184],

$$\frac{\mathrm{d}}{\mathrm{d}t}\hat{\rho} \equiv \hat{\mathcal{L}}\hat{\rho} = \mathrm{i}\left[\hat{\rho}, \hat{H}\right] + \gamma \sum_k \left(\left[\hat{L}_k\hat{\rho}, \hat{L}_k^\dagger\right] + \left[\hat{L}_k, \hat{\rho}\hat{L}_k^\dagger\right]\right), \tag{51}$$

where the Lindblad operators $\hat{L}_k$, describe the coupling between the system and the bath. The Lindlad equation can be numerically solved using tDMRG [185, 186]. The evolution of the density matrix is performed by increasing the size of the Hilbert space and considering the density matrix operator $\hat{\rho}(t)$ as a vector in the enlarged space, whose time evolution is governed by the Liouvillian $\hat{\mathcal{L}}$ (*cf.* (51). In this enlarged Hilbert space the tDMRG method described in the previous section can be applied and it appears that in many cases the entanglement entropy in the operator space, which governs the bond dimension and therefore the efficiency of the method, grows slowly in time due to decoherence effects caused by the Markovian bath. This favorable computational complexity allows to reach the nonequilibrium steady state (NESS) at long times, and to calculate the stationary magnetization and the stationary current [119]. If the bias between left and right leads is small enough, the system is in the linear response regime and the current in the NESS reveals the nature of the transport. Žnidarič *et al.* have used this method to study the dynamical exponent in the random XXZ chain for system sizes up to $L = 400$, arguing in favor of a transition between a diffusive and a subdiffusive regime at weak disorder strength [119]. For strong disorder this method becomes increasingly expensive since the time it takes to reach the stationary state increases.

5.1.5 Dynamical typicality

Quantum typicality can be viewed as a geometrical concept that follows from Lévy's Lemma. This lemma states that for a Lipschitz-continuous function $f : S^{(2n-1)} \to \mathbb{R}$ defined on the surface of a high dimensional sphere, any point $x \in S^{(2n-1)}$ drawn randomly from a uniform distribution on the sphere will yield $f(x)$ exponentially close to the average of f over the surface of the sphere [187].

Since any normalized quantum state in a finite dimensional Hilbert space of dimension $\mathcal{N}$ can be represented as a point on the surface of a $2\mathcal{N}$ dimensional unit hypersphere $S^{(2\mathcal{N}-1)}$, and the trace of an operator $\mathrm{Tr}\,\hat{O}$ can be written as the integral of $\hat{O}$ over the surface of this sphere with respect to the Haar measure, it follows that

the expectation value of $\hat{O}$ for any random pure state $|\psi\rangle$ on the sphere is exponentially close to the value of the trace, if the operator can be represented as a Lipshitz-continuous function on the hypersphere. This is typically the case for local operators. More precisely, the probability to deviate from the trace by more than $\epsilon > 0$ is exponentially small,

$$P\left[\left|\mathrm{Tr}\,\hat{O} - \langle\psi|\,\hat{O}\,|\psi\rangle\right| \geq \epsilon\right] \leq a\mathrm{e}^{-b\mathcal{N}\epsilon^2}, \tag{52}$$

with positive constants a and b. This means that the trace of the operator $\hat{O}$ can be replaced by an expectation value obtained from a random pure state $|\psi\rangle$ to a precision which improves for larger Hilbert space dimension [188–194]. To illustrate its application, we demonstrate how it can be used to calculate a correlation function in the canonical ensemble:

$$C_O^\beta(t) = \frac{1}{Z}\mathrm{Tr}\left(\mathrm{e}^{-\beta\hat{H}}\,\hat{O}\,(t)\,\hat{O}\right) \approx \frac{1}{\langle\beta|\beta\rangle}\left\langle\beta\left|\,\hat{O}\,(t)\,\hat{O}\right|\beta\right\rangle, \tag{53}$$

where β is the inverse temperature. Here we have used the cyclic property of the trace, applied Lévy's lemma substituting the trace by an expectation value of a random state $|\psi\rangle$ and finally defined $|\beta\rangle \equiv \mathrm{e}^{-\frac{\beta}{2}\hat{H}t}|\psi\rangle$ (*cf*. [194]). This state can be efficiently calculated by imaginary time evolution of the pure state $|\psi\rangle$, followed by real time evolution to obtain the correlation function. This task can be performed either by integration of the Schrödinger equation using the recently developed Runge-Kutta schemes [195, 196], or by utilizing the Krylov space technique discussed in the previous section. All these approaches can be applied without full diagonalization of the Hamiltonian and rely solely on the ability to calculate the matrix vector product Hx, which can be achieved even without storing the sparse Hamiltonian matrix H. The memory requirement is thus reduced to the size of a few Hilbert space vectors. We remark that in Ref. [98], we have applied a simplified version of this approach by creating a microcanonical typical state, which we called "energy squeezed state". This state was constructed by applying powers of $(\hat{H}-\sigma)^2$ to a random vector in the Hilbert space to suppress contributions from eigenstates far away from the target energy σ.

5.2 Exact methods for eigenstates calculation

The absence of transport is the defining property that distinguishes the MBL phase from the ergodic phase. Transport can be efficiently studied using the numerical methods described in the previous section. However, the MBL transition can also be viewed as an eigenstate phase transition (*cf*. Ref. [35]), which is characterized by strikingly different properties of the eigenstates of the Hamiltonian in the ergodic and nonergodic phases, but also by different statistical properties of the energy spectrum. To study this aspect numerically, it is therefore important to be able to calculate some or all or the eigenvalues and eigenstates of the Hamiltonian.

Table 2 Comparison of numerical methods for the extraction of high energy eigenstates. The notation is the same as in Table 1, σ^2_{MC} is the target variance of QMC result. The QMC method mentioned here is currently not a strictly exact method [211].

Eigenstates	memory	CPU	L	comment
ED	$\mathcal{O}(\mathcal{N}^2)$	$\mathcal{O}(\mathcal{N}^3)$	≈ 18	shared memory
Shift-Invert	$\mathcal{O}(\mathcal{N}^2)$	$\mathcal{O}(\mathcal{N}^3)$	≈ 22	distributed memory
ES-DMRG	$\mathcal{O}(L\chi^2)$	$\mathcal{O}(L\chi^3)$	≈ 100	MBL only
SI-DMRG	$\mathcal{O}(L\chi^2)$	$\mathcal{O}(L\chi^4)$	≈ 100	MBL only
QMC	$\mathcal{O}(L)$	$\mathcal{O}(\frac{1}{\sigma^2_{\mathrm{MC}}})$	≈ 100	MBL only, approx.

5.2.1 Full diagonalization

Clearly, the first choice to obtain exact high energy eigenstates[9] is the full diagonalization of the Hamiltonian. This is typically done using the standard protocol for dense matrices: First, the Hamiltonian is brought to tridiagonal form by Householder reflections, the tridiagonal matrix is then diagonalized by efficient algorithms, such as the divide and conquer [197] approach or using multiple relatively robust representations [198], and finally the obtained eigenvectors are transformed back to the original basis using the Householder transformations of the first step in inverse order. This recipe is available in highly optimized LAPACK implementations for many architectures, yielding high precision results. Since these methods are based on dense matrices, they require $\mathcal{O}(\mathcal{N}^2)$ memory to store the dense matrix (in addition to $\mathcal{O}(\mathcal{N}^2)$ work space for the divide and conquer algorithm) as well as to store all eigenvectors of the result. The computational complexity is dominated by the Householder step and it scales as $\mathcal{O}(\mathcal{N}^3)$ (cf. Table 2).

[9] This means typically states from the center of the spectrum where the density of states is exponentially large.

5.2.2 Subset diagonalization

For some applications only a few eigenstates and eigenvalues within some interval $[E_-, E_+]$ are required. The *shift-invert* method is the current state-of-the-art method to tackle this problem. It is closely related to inverse iteration and relies on the fact that the extremal eigenvalues of $(\mathsf{H}-\sigma)^{-1}$ correspond to the eigenvalues of H which are closest to the *target energy* σ. Furthermore, while the typical scaling of the level spacing of the original problem is $\mathcal{N}^{-1}$, the level spacing in the corresponding part of the transformed spectrum is $\mathcal{N}$. Therefore standard Krylov space methods, such as the Lanczos algorithm or the Arnoldi iteration can be efficiently used to obtain several of the highest and lowest lying eigenvalues and eigenstates of the transformed problem. The eigenvalues of the transformed problem are trivially transformed back to the original problem and the eigenvectors are invariant under this transformation and therefore are directly obtained.

The hardest part of this procedure is the repeated calculation of the action of $(\mathsf{H}-\sigma)^{-1}$ on vectors during the application of Krylov space methods. This is typically done by first decomposing the Hamiltonian into upper and lower triangular matrices (the LU decomposition) such that $(\mathsf{H}-\sigma)=\mathsf{LU}$ using Gaussian elimination. Subsequently $\mathsf{LU}\mathsf{x}=\mathsf{b}$ is solved, yielding $\mathsf{x}=(\mathsf{H}-\sigma)^{-1}\mathsf{b}$. For the calculation of the LU decomposition, efficient implementations that exploit the sparseness of H are available. For example, for distributed memory machines the MUMPS [199, 200] and SuperLU [201] libraries can be used. The shift-invert technique has been used to map the energy-disorder phase-diagram of the XXZ model (1) by one of us [40].

5.2.3 Excited state DMRG

While matrix product state methods are extremely successful for the study of ground-state properties of one dimensional systems, they were typically not employed to find matrix product state (MPS) representations of highly excited eigenstates of the Hamiltonian, which only recently became of interest in the context of MBL. Due to the area law entanglement of eigenstates in the MBL phase it is natural to expect that such a representation will be efficient. In the ergodic phase, on the other hand it is highly inefficient due to the volume law scaling of entanglement. Recently, several groups have developed methods to find highly excited eigenstates with MPS based methods, which work well in the MBL phase. Yu *et al.* developed SIMPS (shift invert matrix product state method) that relies on the idea of the shift-invert method [202], trying to find an MPS which best approximates the eigenstate of $(\hat{H}-\sigma)^{-1}$ with the largest magnitude eigenvalue. For this purpose, Yu *et al.* propose a method, which is used to iteratively apply $(\hat{H}-\sigma)^{-1}$ to an initial MPS $|\psi_0\rangle$. This iteration is converging exponentially fast (at sufficiently large bond dimension) to an eigenstate of $(\hat{H}-\sigma)^{-1}$ which corresponds to an excited state of the Hamiltonian with an eigenvalue close to σ. The key insight of the method is that the next iteration $|\psi_k\rangle$ could be thought of as a solution of a variational minimization problem $\left\|(\hat{H}-\sigma)|\psi_k\rangle - |\psi_{k-1}\rangle\right\|^2$ where $|\psi_{k-1}\rangle$ corresponds to the previous iteration. The solution of this problem is obtained using an adapted version of the DMRG sweeping protocol. This method was subsequently used by Serbyn *et al.* to study the entanglement spectrum in the MBL phase [203].

As SIMPS relies on a modification of DMRG, a simpler method was proposed to obtain MPS representations of highly excited eigenstates in DMRG [202, 204]. Instead of trying to invert the global Hamiltonian, it is based on the local effective Hamiltonians appearing during the DMRG sweep. The local matrices of the MPS are updated by choosing an excited eigenstate of the local Hamiltonian and yielding an eigenstate of the global Hamiltonian not necessarily close to a target energy. The procedures of selecting the eigenstates of the effective Hamiltonian either relies on choosing the eigenstate with energy closest to the energy of the previous MPS [202], or on the property of the MBL phase that the eigenstates are very close to product states, such that an eigenstate which has the maximal overlap with the MPS of the previous iteration is selected [204]. This approach circumvents the general problem that for large system sizes, the energy level spacing of the full spectrum becomes smaller than machine precision. Other approaches exploit the idea of "spectum folding", noting that the groundstate of $(\hat{H}-\sigma)^2$ corresponds to the eigenstate of $\hat{H}$ with an eigenvalue closest to σ [205, 206]. All these methods are currently employed only in the MBL phase and it is unclear whether they will be useful to study the physics very close to the transition or in the ergodic phase due to the presence of high entanglement entropy. We note that in the fully MBL phase it has been argued that the complete spectrum can be encoded in a single matrix product operator [207–210].

5.2.4 Quantum Monte-Carlo

Quantum Monte-Carlo (QMC) methods are extremely useful to study equilibrium finite temperature physics as well as low temperature properties provided that there is

no sign problem. However, they are not able to resolve single eigenstates which are not groundstates. Inglis and Pollet have recently made progress in this direction by effectively shifting the energies of the original Hamiltonian to make a highly excited eigenstate the new groundstate [211]. This is achieved by exploiting the fact that eigenstates of MBL systems can be labeled by eigenvalues of on extensive number of conserved quasilocal quantities [212, 213]. This method is conceptually new and very promising, although its current implementation relies on an approximate construction of the quasilocal conserved operators with constraints on their analytic form to make them compatible with the worm algorithm. By construction, this method is only useful to study the MBL phase.

5.3 Approximate method: perturbation theory

All numerically exact methods have strong size or time constraints, which result in finite size effects, especially in the limit of weak disorder. These constraints are even more pronounced in higher dimensions, where currently there are no efficient methods for an exact study of nonequilibrium dynamics. Access to larger systems and longer times can be gained by utilizing approximate methods. Below we survey one such approach which was successfully applied for the study of transport in one-dimensional [31] and a two dimensional system by one of us [114].

For the MBL problem this method was introduced in the work of Basko, Aleiner and Altshuler [18]. The method is *perturbative* in the interaction strength and as was demonstrated by one of us, is able to *quantitatively* reproduce numerically exact results in the limit of large disorder. For very weak disorder, the method becomes increasingly unreliable and tends to overestimate the relaxation in the system [31, 114]. We note that while perturbation theory is clearly an analytical tool, its numerical implementation requires the solution of certain numerical difficulties (for details see [214]). The quantities of interest are one particle correlation functions,

$$\begin{aligned} G_{ij}^{>}\left(t;t'\right) &= -i\mathrm{Tr}\left(\hat{\rho}_0 \hat{c}_i\left(t\right)\hat{c}_j^{\dagger}\left(t'\right)\right) \\ G_{ij}^{<}\left(t;t'\right) &= i\mathrm{Tr}\left(\hat{\rho}_0 \hat{c}_j^{\dagger}\left(t'\right)\hat{c}_i\left(t\right)\right), \end{aligned} \tag{54}$$

where $\hat{\rho}_0$ is the initial density matrix and $\hat{c}_j^{\dagger}$ creates a spinless fermion at site j. For a noninteracting initial density matrix, the Green's functions obey the Kadanoff–Baym equations of motion [215],

$$\begin{aligned} i\partial_t G^{\gtrless}\left(t,t'\right) &= \left(\hat{h}_0 + \Sigma^{HF}\left(t\right)\right) G^{\gtrless}\left(t,t'\right) \\ &\quad + \int_0^t \Sigma^{R}\left(t,t_2\right) G^{\gtrless}\left(t_2,t'\right) \mathrm{d}t_2 \\ &\quad + \int_0^{t'} \Sigma^{\gtrless}\left(t,t_2\right) G^{A}\left(t_2,t'\right) \mathrm{d}t_2, \end{aligned} \tag{55}$$

where spatial indices and summations are suppressed for clarity, $\hat{h}_{0,nm}$ is the one particle Hamiltonian, $\Sigma^{HF}(t)$, $\Sigma^{\gtrless}(t)$ are the Hartree-Fock, greater and lesser self-energies of the problem respectively; and the superscripts 'R' and 'A' represent retarded and advanced Green's functions and self-energies, which are defined as

$$\begin{aligned} \Sigma^{R}\left(t,t_2\right) &= \theta\left(t-t_2\right)\left(\Sigma^{>}\left(t,t_2\right) - \Sigma^{<}\left(t,t_2\right)\right) \\ G^{A}\left(t_2,t'\right) &= -\theta\left(t'-t_2\right)\left(G^{>}\left(t_2,t'\right) - G^{<}\left(t_2,t'\right)\right). \end{aligned} \tag{56}$$

Since the exact form of the self-energies is normally unknown, they are commonly approximated up to some order in the small parameter of the problem. For the problem which is the subject of this review the natural small parameter is $\lambda \equiv U/\delta$ where U is the interaction strength and δ is the typical energy difference of nearby localized single-particle states $\delta \equiv \Delta/\xi$. Here Δ is the single-particle bandwidth and ξ is the single-particle localization length. To second order in λ a particularly useful approximation is the self-consistent second-Born approximation,

$$\begin{aligned} \Sigma_{ij}^{HF}\left(t\right) &= -i\delta_{ij}\sum_k V_{ik} G_{kk}^{<}\left(t;t\right) + iV_{ij}G_{ij}^{<}\left(t;t\right) \\ \Sigma_{ij}^{>}\left(t,t'\right) &= \sum_{k,l} V_{il}V_{jk}G_{kl}^{<}\left(t',t\right) \\ &\quad \times\left[G_{lk}^{>}\left(t,t'\right)G_{ij}^{>}\left(t,t'\right) - G_{lj}^{>}\left(t,t'\right)G_{ik}^{>}\left(t,t'\right)\right], \end{aligned} \tag{57}$$

where $V_{ij} = V(\delta_{i,j+1} + \delta_{i,j-1})$ is the interaction potential. Using this approximation one can write a closed form equation for the correlation functions (54), which is then solved numerically. This method requires a memory which scales like $\mathcal{O}(L^2 N_t^2)$, where N_t is the number of time steps required to solve (55) to predetermined precision. The computational complexity of this method scales like $\mathcal{O}(L^3 N_t^3)$, and could be further reduced to $\mathcal{O}(L^3 N_t^2)$ by making additional approximations [216–218]. For more technical details on this method as also to detailed comparison to exact methods the the reader is referred to Refs. [31, 114, 218].

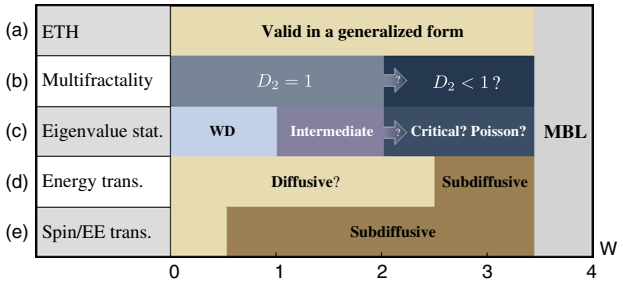

Figure 2 A visual summary of current results and open questions on the ergodic phase of the XXZ model (1) with $J_z = 1$. Different color patches represent different phases as suggested by various studies. The locations of transitions or crossovers between the different phases are presented only approximately and are displayed as sharp for better readability. Question marks represent open questions and arrows indicate that some studies suggest that the phase shrinks to the critical point $W_c \approx 3.7$ in the thermodynamic limit. **(a)** The validity of ETH was studied in Refs. [98, 137], **(b)** the generalized fractal dimensions $D_{1,2}$ were studied in Refs. [40, 90, 91], **(c)** a detailed study of the eigenvalue statistics was done in Refs. [70, 91], **(d)** energy transport was studied in Ref. [147], **(e)** spin transport and entanglement spreading was studied in Refs. [32, 33, 126, 137, 146].

6 Discussion and open questions

In the previous sections we reviewed in detail the current knowledge of the ergodic phase at weak disorder, preceding the MBL transition. Here, we will identify some important open questions and discuss the progress that has been made towards answering them. In Fig. 2 we present a visual summary of the results as also some of the open questions. It is apparent, that while recent works identified fascinating possible scenarios for the rich physics of the ergodic phase, the overall picture is not yet settled. Future works in this field will have to clarify how the observed phenomenology evolves as a function of system size to put existing contradictions into perspective.

6.1 Subdiffusion and the subdiffusion to diffusion transition

While the MBL phase can be defined by an absence of transport, the nature of transport in the ergodic phase is not a priori clear. Many numerical studies have addressed this question after first evidence for subdiffusive transport in a one-dimensional XXZ model was found [32, 33]. The results of most numerical studies are consistent with the interpretation that at intermediate disorder $1 \lesssim W \lesssim 3.7$ spin transport is subdiffusive and the entanglement growth is sublinear [32, 33, 126, 137, 146], with a continuously varying dynamical exponent z, which diverges at the MBL transition. In Ref. [147] it was argued that for $1 \lesssim W \lesssim 2.5$ energy transport is diffusive while spin transport is subdiffusive. This study however is in contradiction with Ref. [137], since if true asymptotically in time, it would suggest that energy was transported faster than information (entanglement entropy). For very weak disorder, $W < 1$, some studies yet find subdiffusive spin transport [137], while others argue in favor of a transition to diffusion [33, 119]. Currently, the most compelling evidence stems from the study of an *open* XXZ chain with system sizes up to $L = 400$ by Žnidarič *et al.* [119]. This work argues in favor of a transition between diffusive and subdiffusive behavior at $W \approx 0.6$. While this work cannot rule out weak subdiffusive transport for $W < 0.6$, which might occur for even larger system sizes (see right panel of Fig. 1, and discussion at the end of Sec. 3.3.6), it points out that ED studies in this region of parameters are subject to severe finite size effects. Interestingly, in this region, $W < 0.6$ the fluctuations of local operators in the eigenbasis of the Hamiltonian are perfectly Gaussian, verifying exactly the ETH ansatz [97, 98]. However currently no direct connection between the nature of transport and the shape of the probability distributions is known and we can only speculate that such perfectly Gaussian distributions are a sign for diffusion, while heavily tailed non-Gaussian distributions may signal subdiffusion. The situation in dimensions higher than one is less clear, since numerically addressing transport for $d \geq 2$ remains very challenging. Algorithmic progress and input from experiments is required to clarify the nature of transport in this case. Currently there is only one numerical study which points towards subdiffusion in two dimensions based on perturbation theory (*cf.* Sec. 5.3) [114].

This seemingly clear picture of transport in one-dimensional systems is disturbed if the numerical evidence is quantitatively compared. We have presented a comparison of recent numerical estimates of the dynamical exponent obtained by various methods. By looking on Fig. 1 it is obvious that the results match only qualitatively, moreover some commonly used relations between the exponents [*cf.* Eq. (33)] do not hold. While this might indicate that some of these relations should be reconsidered, the observed disagreement between the exponents could also follow from the difficulty of extracting dynamical exponents from numerical calculations on finite systems. In fact, a very recent work evaluated the spread of spin perturbations starting from initial conditions with fixed energy density [219]. In this work a convergent (with system size) dynamical exponent could

not be obtained and it was argued that the observed subdiffusion is a transient [219]. Asymptotic diffusion and finite dc conductivity in the whole ergodic phase were also found in ac conductivity studies [121, 122], using system sizes up to $L = 28$ similar to the studies which observe subdiffusion. Future work will have to resolve this contradiction.

6.2 Existence of the "bad metal"

The observation of intermediate level statistics as well as of multifractal distributions of local operators at disorder strengths $W \gtrsim 2$ [70, 90] is consistent with the prediction of the existence of a delocalized, `nonergodic` phase (dubbed "bad metal" by Altshuler [74]) for disorder strengths below the MBL transition [73]. However, the question whether this phase shrinks in the thermodynamic limit to a critical point or remains of finite extent in the parameter space is still open [90, 91]. Large scale studies on random regular graphs (RRGs) seem to point out that this phase disappears in the thermodynamic limit [85–87], although there is also no consensus here [80–88]. Moreover while both problems are related, it is not clear a priori that results from RRGs apply for physical models.

The multifractal nature of this phase suggests that it might be related to the observed subdiffusion, and could also explain the poor agreement between the various dynamical exponents, as presented in the summary of Sec. 3.3 (see Fig. 1). While a direct relation between multifractality in the many-body space and real space subdiffusion was not established, a step in this direction was performed in Refs. [70, 90, 98]. There are however a few problems with this interpretation: (i) subdiffusion appears to persist in the thermodynamic limit [119] while the "bad metal" seems to shrink in this limit [90], (ii) looking at Fig. 2 it is clear that the extent of observed subdiffusion is much larger then the extent of the observed multifractality (iii) in this region the definitions of ergodicity via ETH and `ergodicity`(via eigenvector statistics) do not agree, suggesting that the definitions of ergodicity as discussed in Sec. 3.1 are not equivalent.

Another interesting question is whether there is a relation between the "bad metal" and the Griffiths effects picture presented in Sec. 4.

6.3 Mechanism of subdiffusive transport

Even though the numerical evidence is not univocal, the existence of a subdiffusive regime is certainly a valid scenario consistent with many numerical studies. The proposed mechanism for subdiffusive transport, dubbed Griffiths effects, is the existence of rare insulating regions which serve as bottlenecks for the transport of particles and entanglement [33, 133]. While this mechanism is difficult to test numerically, it seems consistent with spatial variations in the entanglement structure as observed numerically [97, 104, 107]. However, other indirect tests of the predictions of the Griffiths picture reveal several issues: (i) it predicts asymptotic diffusion in dimensions higher then one (*cf*. the review [36]), which seems to contradict the observation of subdiffusion in two dimensions [114] (ii) it predicts diffusion for quasiperiodic potentials, although sublinear entanglement growth was observed for the Aubry-André model in Ref. [220] as well as subdiffusive transport in Refs. [221, 222] (iii) Griffiths effects are expected to be subdominant far from the MBL transition, which is in contrast to the extended subdiffusive phase found in most studies. Due to the above, we feel that Griffiths picture may have to be refined in future works. In particular its relation to observed signatures of multifractality has to be better understood.

6.4 Relation to classical disordered models

An important point that we did not discuss in this review is the connection between the quantum and classical disordered models. The pertinent question in the context of the ergodic phase is to which extent the ergodic phase, which is the subject of this review, can be considered classical. A pioneering study in this direction suggests that classical disordered models are diffusive [66]. We refer the reader on a recent review on this subject [223].

The MBL transition is in many ways similar to the glass transition [18]. In particular commonly used MBL models, such as (1) and (4), are superficially reminiscent of spin-glass models. Both have quenched disorder and a *finite* temperature ergodic–nonergodic transition. However while much of the phenomenology is similar, there are important differences. The spin glass transition is a thermodynamic phase transition which occurs in a presence of an external heat bath [224], while the MBL transition does not appear to have a thermodynamic signature and occurs only for *isolated* systems [18]. One of the most interesting questions in this context, is whether the ergodicity breaking mechanisms of spin glasses and MBL are somehow related.

The relation to structural glasses is more remote, due to absence of quenched disorder in the structural glasses

models. Attempts to find a stable MBL phase for disorder free, translationally invariant models were unsuccessful [89, 225–235]. Notwithstanding, the ergodic phase which is the subject of this review, shares many properties with supercooled liquids [112]. To point out these parallels, we have used notation borrowed from the structural glasses community in our discussion of the dynamical properties in Sec, 3.3. Similarly to the supercooled liquids the ergodic phase thermalizes, and the relaxation of density (spin) autocorrelation functions is subexponential with a relaxation time which diverges at the transition. Interestingly, the theory of the MBL transition as established in Ref. [18] is also reminiscent of the mode-coupling theory, which works remarkably well for structural glasses [236]. Deeper connections between the two fields should definitely be explored in future works.

6.5 Summary

In this review we surveyed the features of the ergodic phase, which occurs in generic interacting systems with sufficiently weak quenched disorder. We have explained in which sense this phase could be considered ergodic, and elaborated on the different notions of ergodicity in this context. We presented the peculiar static and dynamical properties of this phase, which is characterized by intermediate eigenvalue statistics, signatures of multifractality and the emergence of power-laws for almost any dynamical property, including the growth of the entanglement entropy. We have explained the phenomenological rare-region picture (the Griffiths picture), and its predictions on the relations between the different power-law exponents, as also the numerical verification of these predictions. Finally, we presented all available numerically exact and approximate methods for the exploration of this phase and finished the review with discussion of some of the pertinent open questions.

Acknowledgments. We are grateful to Ilia Khait and Marko Žnidarič for sharing their original data. YB acknowledges funding from the Simons Foundation (#454951, David R. Reichman). DJL was supported by the Gordon and Betty Moore Foundation's EPiQS Initiative through Grant No. GBMF4305 at the University of Illinois. This research is part of the Blue Waters sustained-petascale computing project, which is supported by the National Science Foundation (awards OCI-0725070 and ACI-1238993) and the state of Illinois. Blue Waters is a joint effort of the University of Illinois at Urbana-Champaign and its National Center for Supercomputing Applications.

Appendix A: Relation between the mean-square displacement and the current-current correlation functions

In this section we derive a general relation between the correlations of a conserved quantity and the correlations of the corresponding current, which could be useful to application well beyond the scope of this review.

We focus on Hamiltonians which conserve the quantity, $\hat{Q} = \sum_{m=1}^{L} \hat{n}_m$, namely $[\hat{H}, \hat{Q}] = 0$, and for which the following continuity equation applies,

$$\frac{\partial \hat{n}_k}{\partial t} = \Delta \hat{j}_k, \tag{A1}$$

where $\Delta j_k \equiv j_k - j_{k-1}$ is the backward discrete derivative. We define the means square displacement (MSD) of the excitation in this density to be

$$x^2(t) = \frac{1}{L} \sum_{k=1}^{L} \sum_{l=1}^{L} (k-l)^2 \,\mathrm{Re}\, \langle \delta \hat{n}_k(t)\, \delta \hat{n}_l \rangle , \tag{A2}$$

where $\langle . \rangle$ is the equilibrium average and $\delta \hat{n}_k(t) \equiv \hat{n}_k(t) - \langle \hat{n}_k \rangle$. We note the following identity,

$$\begin{aligned} \left\langle \left(\hat{n}_k(t) - \hat{n}_k\right)\left(\hat{n}_l(t) - \hat{n}_l\right)\right\rangle &= 2\langle \delta \hat{n}_k \delta \hat{n}_l \rangle \\ &\quad - \langle \delta \hat{n}_k(t)\, \delta \hat{n}_l + \delta \hat{n}_k \delta \hat{n}_l(t) \rangle, \end{aligned} \tag{A3}$$

which is true for expectation with respect to the equilibrium state. To calculate MSD we multiply by $(k-l)^2$ and sum twice over the lattice, which gives,

$$\begin{aligned} &x^2(t) - x^2(0) \\ &\quad = -\frac{1}{2L} \sum_{k,l=1}^{L} (k-l)^2 \left\langle \left(\hat{n}_k(t) - \hat{n}_k\right)\left(\hat{n}_l(t) - \hat{n}_l\right)\right\rangle . \end{aligned} \tag{A4}$$

Using the continuity equation we can write,

$$\hat{n}_k(t) - \hat{n}_k = \int_0^t \mathrm{d}\bar{t}\, \Delta \hat{j}_k(\bar{t}) , \tag{A5}$$

such that

$$\begin{aligned} x^2(t) - x^2(0) = -\frac{1}{2L} \int_0^t \mathrm{d}t_1 \int_0^t \mathrm{d}t_2 \times \\ \times \sum_{k,l=1}^{L} (k-l)^2 \left\langle \Delta \hat{j}_k(t_1)\, \Delta \hat{j}_l(t_2) \right\rangle . \end{aligned}$$

Taking a partial sum twice and assuming periodic boundary conditions (or alternatively neglecting the

boundary terms) gives,

$$x^2(t) - x^2(0) = \frac{1}{L}\int_0^t \mathrm{d}t_1 \int_0^t \mathrm{d}t_2 \left\langle \hat{J}(t_1)\,\hat{J}(t_2)\right\rangle, \tag{A7}$$

where $\hat{J}(t) = \sum_{k=1}^{L} \hat{j}_k(t)$ is the total current. Since any correlation function in equilibrium depends only on the time difference we change the variables to $\tau = t_1 - t_2$, and $t_1 = t_1$ which has an unity Jacobian and the following transformation of the integration boundaries,

$$x^2(t) - x^2(0) = \frac{2}{L}\int_0^t \mathrm{d}t_1 \int_0^{t_1} \mathrm{d}\tau \left\langle \hat{J}(\tau)\,\hat{J}(0)\right\rangle, \tag{A8}$$

which could also be written as,

$$\left\langle \hat{J}(t)\,\hat{J}(0)\right\rangle = \frac{\mathrm{d}^2}{\mathrm{d}t^2} x^2(t), \tag{A9}$$

which is very similar to its classical form. Taking the Fourier transform we get the relation between the corresponding frequency dependent diffusion coefficient and the MSD (Eq. (14)),

$$D(\omega) = -\omega^2 \int_{-\infty}^{\infty} \mathrm{d}t\, x^2(t)\, \mathrm{e}^{\mathrm{i}\omega t}. \tag{A10}$$

We note that this derivation assumes only the continuity equation (A1), periodic boundary conditions and an expectation value with respect to the thermal state. It does not assume linear response and any knowledge about the Hamiltonian except of the existence of the conserved quantity. It also does not assume any specific form of the conserved quantity or the corresponding current.

Key words. Many-body localization, Ergodicity, eigenstate thermalization hypothesis, Subdiffusion, anomalous thermalization, disorder.

David J. Luitz obtained a doctoral degree in theoretical physics at the University of Würzburg in 2013. He then moved to Toulouse, France for his first postdoctoral position in the french CNRS. In 2015, he joined the University of Illinois at Urbana-Champaign as a Gordon and Betty Moore Postdoctoral fellow and moved to Technische Universität München as a Marie Skłodowska Curie fellow in 2017. His research is focussed on the numerical study of strongly correlated quantum systems in and out-of equilibrium.

Yevgeny Bar Lev received his PhD in theoretical physics from Technion in 2010. After a postdoctoral appointment at Technion, he moved to Columbia University as a Fulbright postdoctoral fellow in 2012. His interests span disordered and interacting systems as also nonequilibrium dynamics.

References

[1] L. Boltzmann, Crelle's J. **98**, 68 (1884).
[2] J. von Neumann, Z. Phys. **57**, 30 (1929).
[3] J. von Neumann, The European Physical Journal H **35**, 201 (2010).
[4] M. V. Berry, J. Phys. A. Math. Gen. **10**, 2083 (1977).
[5] P. Pechukas, Phys. Rev. Lett. **51**, 943 (1983).
[6] P. Pechukas, J. Phys. Chem. **88**, 4823 (1984).
[7] M. Feingold, N. Moiseyev, and A. Peres, Phys. Rev. A **30**, 509 (1984).
[8] M. Feingold, N. Moiseyev, and A. Peres, Chem. Phys. Lett. **117**, 344 (1985).
[9] M. Feingold and A. Peres, Phys. Rev. A **34**, 591 (1986).
[10] A. Peres, Phys. Rev. A **30**, 504 (1984).
[11] A. Peres, Phys. Rev. A **30**, 1610 (1984).
[12] R. V. Jensen and R. Shankar, Physical Review Letters **54**, 1879 (1985).
[13] J. M. Deutsch, Phys. Rev. A **43**, 2046 (1991).
[14] M. Srednicki, Phys. Rev. E **50**, 888 (1994).
[15] M. Srednicki, J. Phys. A. Math. Gen. **29**, L75 (1996).
[16] M. Srednicki, J. Phys. A. Math. Gen. **32**, 1163 (1999).
[17] N. Goldenfeld, Lectures on Phase Transitions and the Renormalization Group, Frontiers in physics (Addison-Wesley, Advanced Book Program, 1992).
[18] D. Basko, I. L. Aleiner, and B. L. Altshuler, Ann. Phys. (N. Y). **321**, 1126 (2006).
[19] J. Z. Imbrie, J. Stat. Phys. **163**, 998 (2016).
[20] J. Z. Imbrie, Phys. Rev. Lett. **117**, 027201 (2016).
[21] D. M. Basko, I. L. Aleiner, and B. L. Altshuler, Phys. Rev. B **76**, 052203 (2007).
[22] M. Ovadia, D. Kalok, I. Tamir, S. Mitra, B. Sacépé, and D. Shahar, Sci. Rep. **5**, 13503 (2015).
[23] M. Schreiber, S. S. Hodgman, P. Bordia, H. P. Luschen, M. H. Fischer, R. Vosk, E. Altman, U. Schneider, and I. Bloch, Science **349**, 842 (2015).
[24] P. Bordia, H. P. Lüschen, S. S. Hodgman, M. Schreiber, I. Bloch, and U. Schneider, Phys. Rev. Lett. **116**, 140401 (2016).
[25] J. Smith, A. Lee, P. Richerme, B. Neyenhuis, P. W. Hess, P. Hauke, M. Heyl, D. A. Huse, and C. Monroe, Nat. Phys. **12**, 907 (2016).

[26] J.-y. Choi, S. Hild, J. Zeiher, P. Schauss, A. Rubio-Abadal, T. Yefsah, V. Khemani, D. A. Huse, I. Bloch, and C. Gross, Science **352**, 1547 (2016).
[27] E. Altman and R. Vosk, Annu. Rev. Condens. Matter Phys. **6**, 383 (2015).
[28] R. Nandkishore and D. A. Huse, Annu. Rev. Condens. Matter Phys. **6**, 15 (2015).
[29] R. Vasseur and J. E. Moore, J. Stat. Mech. Theory Exp. **2016**, 064010 (2016).
[30] P. W. Anderson, Phys. Rev. **109**, 1492 (1958).
[31] Y. Bar Lev and D. R. Reichman, Phys. Rev. B **89**, 220201 (2014).
[32] Y. Bar Lev, G. Cohen, and D. R. Reichman, Phys. Rev. Lett. **114**, 100601 (2015).
[33] K. Agarwal, S. Gopalakrishnan, M. Knap, M. Müller, and E. Demler, Phys. Rev. Lett. **114**, 160401 (2015).
[34] J. Z. Imbrie, V. Ros, and A. Scardicchio, Ann. Phys. (Berlin) **529**, 1600278 (2017).
[35] S. A. Parameswaran, A. C. Potter, and R. Vasseur, Ann. Phys. (Berlin) **529**, 1600302 (2017).
[36] K. Agarwal, E. Altman, E. Demler, S. Gopalakrishnan, D. A. Huse, and M. Knap, Ann. Phys. (Berlin) **529**, 1600326 (2017).
[37] A. Haldar and A. Das, Ann. Phys. (Berlin) **529**, 1600333 (2017).
[38] D.-L. Deng, S. Ganeshan, X. Li, R. Modak, S. Mukerjee, and J. H. Pixley, Ann. Phys. (Berlin) **529**, 1600399 (2017).
[39] P. Jordan and E. Wigner, Z. Phys. **47**, 631 (1928).
[40] D. J. Luitz, N. Laflorencie, and F. Alet, Phys. Rev. B **91**, 081103 (2015).
[41] A. C. Potter and R. Vasseur, Phys. Rev. B **94**, 224206 (2016).
[42] P. Prelovšek, O. S. Barišić, and M. Žnidarič, Phys. Rev. B **94**, 241104 (2016).
[43] L. D'Alessio and A. Polkovnikov, Ann. Phys. (N. Y). **333**, 19 (2013).
[44] P. Ponte, A. Chandran, Z. Papić, and D. A. Abanin, Ann. Phys. (N. Y.) **353**, 196 (2015).
[45] A. Lazarides, A. Das, and R. Moessner, Physical Review Letters **115**, 030402 (2015).
[46] D. A. Abanin, W. De Roeck, and F. Huveneers, Phys. Rev. Lett. **115**, 256803 (2015).
[47] P. Ponte, Z. Papić, F. Huveneers, and D. A. Abanin, Physical Review Letters **114**, 140401 (2015).
[48] D. A. Abanin, W. De Roeck, and F. Huveneers, Annals of Physics **372**, 1 (2016).
[49] P. Bordia, H. Lüschen, U. Schneider, M. Knap, and I. Bloch, Periodically driving a many-body localized quantum system, (2016), arXiv:1607.07868.
[50] J. Rehn, A. Lazarides, F. Pollmann, and R. Moessner, Phys. Rev. B **94**, 020201 (2016).
[51] L. Zhang, V. Khemani, and D. A. Huse, Phys. Rev. B **94**, 224202 (2016).
[52] S. Goldstein, J. L. Lebowitz, R. Tumulka, and N. Zanghì, Eur. Phys. J. H **35**, 173 (2010).
[53] O. Bohigas, M.-J. Giannoni, and C. Schmit, in Quantum Chaos Stat. Nucl. Phys. (1986) pp. 18–40.
[54] A. Andreev, O. Agam, B. Simons, and B. L. Altshuler, Phys. Rev. Lett. **76**, 3947 (1996).
[55] G. Montambaux, D. Poilblanc, J. Bellissard, and C. Sire, Phys. Rev. Lett. **70**, 497 (1993).
[56] D. Poilblanc, T. Ziman, J. Bellissard, F. Mila, and G. Montambaux, EPL **22**, 537 (1993).
[57] R. Berkovits, EPL **25**, 681 (1994).
[58] R. Berkovits and Y. Avishai, J. Phys. Condens. Matter **8**, 389 (1996).
[59] P. Jacquod and D. L. Shepelyansky, Phys. Rev. Lett. **79**, 1837 (1997).
[60] B. Georgeot and D. L. Shepelyansky, Physical Review Letters **81**, 5129 (1998).
[61] Y. Avishai, J. Richert, and R. Berkovits, Phys. Rev. B **66**, 2 (2002).
[62] L. F. Santos, J. Phys. A. Math. Gen. **37**, 4723 (2004).
[63] L. F. Santos, G. Rigolin, and C. O. Escobar, Phys. Rev. A **69**, 042304 (2004).
[64] V. Oganesyan and D. A. Huse, Phys. Rev. B **75**, 155111 (2007).
[65] T. Guhr, A. Müller-Groeling, and H. A. Weidenmüller, Phys. Rep. **299**, 189 (1998).
[66] V. Oganesyan, A. Pal, and D. A. Huse, Phys. Rev. B **80**, 115104 (2009).
[67] Y. Y. Atas, E. Bogomolny, O. Giraud, and G. Roux, Phys. Rev. Lett. **110**, 084101 (2013).
[68] F. J. Dyson, J. Math. Phys. **3**, 1191 (1962).
[69] J. T. Chalker, I. V. Lerner, and R. A. Smith, Journal of Mathematical Physics **37**, 5061 (1996).
[70] M. Serbyn and J. E. Moore, Phys. Rev. B **93**, 041424 (2016).
[71] F. Evers and A. Mirlin, Rev. Mod. Phys. **80**, 1355 (2008).
[72] C. L. Bertrand and A. M. García-García, Phys. Rev. B **94**, 144201 (2016).
[73] B. L. Altshuler, Y. Gefen, A. Kamenev, and L. S. Levitov, Phys. Rev. Lett. **78**, 2803 (1997).
[74] B. L. Altshuler, "Many-body localization," (2010).
[75] R. Ketzmerick, K. Kruse, S. Kraut, and T. Geisel, Phys. Rev. Lett. **79**, 1959 (1997).
[76] T. Ohtsuki and T. Kawarabayashi, J. Phys. Soc. Japan **66**, 314 (1997).
[77] Y. Y. Atas and E. Bogomolny, Physical Review E **86**, 021104 (2012).
[78] D. J. Luitz, F. Alet, and N. Laflorencie, Physical Review Letters **112**, 057203 (2014).
[79] F. Borgonovi, F. Izrailev, L. Santos, and V. Zelevinsky, Phys. Rep. **626**, 1 (2016).
[80] G. Biroli, A. C. Ribeiro-Teixeira, and M. Tarzia, Difference between level statistics, ergodicity and localization transitions on the bethe lattice, (2012), arXiv:1211.7334.
[81] A. De Luca, A. Scardicchio, V. E. Kravtsov, and B. L. Altshuler, Support set of random wave-functions on the bethe lattice, (2013), arXiv:1401.0019.
[82] A. De Luca, B. L. Altshuler, V. E. Kravtsov, and A. Scardicchio, Phys. Rev. Lett. **113**, 046806 (2014).
[83] V. E. Kravtsov, I. M. Khaymovich, E. Cuevas, and M. Amini, New J. Phys. **17**, 122002 (2015).

[84] D. Facoetti, P. Vivo, and G. Biroli, EPL **115**, 47003 (2016).
[85] K. S. Tikhonov, A. D. Mirlin, and M. A. Skvortsov, Phys. Rev. B **94**, 220203 (2016).
[86] K. S. Tikhonov and A. D. Mirlin, Phys. Rev. B **94**, 184203 (2016).
[87] I. García-Mata, O. Giraud, B. Georgeot, J. Martin, R. Dubertrand, and G. Lemarié, Scaling theory of the anderson transition in random graphs: ergodicity and universality, (2016), arXiv:1609.05857.
[88] B. L. Altshuler, E. Cuevas, L. B. Ioffe, and V. E. Kravtsov, Phys. Rev. Lett. **117**, 156601 (2016).
[89] M. Pino, L. B. Ioffe, and B. L. Altshuler, Proc. Nat. Acad. Sci. **113**, 536 (2016).
[90] M. Serbyn, Z. Papić, and D. A. Abanin, Thouless energy and multifractality across the many-body localization transition, (2016), arXiv:1610.02389.
[91] E. J. Torres-Herrera and L. F. Santos, Ann. Phys. (Berlin) **529**, 1600284 (2017).
[92] C. Monthus, J. Stat. Mech. Theory Exp. **2016**, 073301 (2016).
[93] M. Rigol, V. Dunjko, and M. Olshanii, Nature **452**, 854 (2008).
[94] L. D'Alessio, Y. Kafri, A. Polkovnikov, and M. Rigol, Adv. Phys. **65**, 239 (2016).
[95] C. Gogolin and J. Eisert, Reports Prog. Phys. **79**, 056001 (2016).
[96] A. Pal and D. A. Huse, Phys. Rev. B **82**, 174411 (2010).
[97] D. J. Luitz, Phys. Rev. B **93**, 134201 (2016).
[98] D. J. Luitz and Y. Bar Lev, Phys. Rev. Lett. **117**, 170404 (2016).
[99] N. Laflorencie, Physics Reports Quantum entanglement in condensed matter systems **646**, 1 (2016).
[100] B. Bauer and C. Nayak, J. Stat. Mech. Theory Exp. **2013**, P09005 (2013).
[101] J. A. Kjäll, J. H. Bardarson, and F. Pollmann, Phys. Rev. Lett. **113**, 107204 (2014).
[102] R. Vosk, D. A. Huse, and E. Altman, Phys. Rev. X **5**, 031032 (2015).
[103] A. C. Potter, R. Vasseur, and S. A. Parameswaran, Phys. Rev. X **5**, 031033 (2015).
[104] X. Yu, D. J. Luitz, and B. K. Clark, Phys. Rev. B **94**, 184202 (2016).
[105] V. Khemani, S. P. Lim, D. N. Sheng, and D. A. Huse, Critical Properties of the Many-Body Localization Transition, (2016), arXiv:1607.05756.
[106] T. Grover, Certain general constraints on the many-body localization transition, (2014), arXiv:1405.1471.
[107] S. Bera and A. Lakshminarayan, Phys. Rev. B **93**, 134204 (2016).
[108] G. De Tomasi, S. Bera, J. H. Bardarson, and F. Pollmann, Phys. Rev. Lett. **118**, 016804 (2017).
[109] A. Karahalios, A. Metavitsiadis, X. Zotos, A. Gorczyca, and P. Prelovšek, Phys. Rev. B **79**, 024425 (2009).
[110] T. C. Berkelbach and D. R. Reichman, Phys. Rev. B **81**, 224429 (2010).
[111] O. S. Barišić and P. Prelovšek, Phys. Rev. B **82**, 161106 (2010).
[112] K. Binder and W. Kob, Glassy Materials and Disordered Solids: An Introduction to Their Statistical Mechanics (World Scientific Publishing Company, 2005) p. 452.
[113] J. T. Edwards and D. Thouless, J. Phys. C Solid State Phys. **5**, 807 (1972).
[114] Y. Bar Lev and D. R. Reichman, EPL **113**, 46001 (2016).
[115] H. Scher and M. Lax, Phys. Rev. B **7**, 4491 (1973).
[116] S. Gopalakrishnan, M. Müller, V. Khemani, M. Knap, E. A. Demler, and D. A. Huse, Phys. Rev. B **92**, 104202 (2015).
[117] R. Kubo, J. Phys. Soc. Japan **12**, 570 (1957).
[118] M. Kozarzewski, P. Prelovšek, and M. Mierzejewski, Phys. Rev. B **93**, 235151 (2016).
[119] M. Žnidarič, A. Scardicchio, and V. K. Varma, Phys. Rev. Lett. **117**, 040601 (2016).
[120] S. Gopalakrishnan, M. Knap, and E. Demler, Phys. Rev. B **94**, 094201 (2016).
[121] R. Steinigeweg, J. Herbrych, F. Pollmann, and W. Brenig, Phys. Rev. B **94**, 180401 (2016).
[122] O. S. Barišić, J. Kokalj, I. Balog, and P. Prelovšek, Phys. Rev. B **94**, 045126 (2016).
[123] P. Prelovšek and J. Herbrych, Dynamical structure factor in disordered model of interacting fermions, (2016), arXiv:1609.05450.
[124] D. Thouless and S. Kirkpatrick, J. Phys. C Solid State Phys. **14**, 235 (1981).
[125] Y. Imry, Introduction to Mesoscopic Physics (Mesoscopic Physics and Nanotechnology) (Oxford University Press, USA, 2008) p. 252.
[126] I. Khait, S. Gazit, N. Y. Yao, and A. Auerbach, Phys. Rev. B **93**, 224205 (2016).
[127] S. F. Edwards and P. W. Anderson, J. Phys. F Met. Phys. **5**, 965 (1975).
[128] D. A. Huse, R. Nandkishore, V. Oganesyan, A. Pal, and S. L. Sondhi, Phys. Rev. B **88**, 014206 (2013).
[129] D. Pekker, G. Refael, E. Altman, E. A. Demler, and V. Oganesyan, Phys. Rev. X **4**, 011052 (2014).
[130] R. Vasseur, A. J. Friedman, S. A. Parameswaran, and A. C. Potter, Phys. Rev. B **93**, 134207 (2016).
[131] C. Monthus, Journal of Statistical Mechanics: Theory and Experiment **2016**, 033113 (2016).
[132] S. Alexander, J. Bernasconi, W. R. Schneider, and R. Orbach, Rev. Mod. Phys. **53**, 175 (1981).
[133] S. Gopalakrishnan, K. Agarwal, E. A. Demler, D. A. Huse, and M. Knap, Phys. Rev. B **93**, 134206 (2016).
[134] S. Iyer, V. Oganesyan, G. Refael, and D. A. Huse, Phys. Rev. B **87**, 134202 (2013).
[135] E. J. Torres-Herrera and L. F. Santos, Phys. Rev. B **92**, 014208 (2015).
[136] M. Mierzejewski, J. Herbrych, and P. Prelovšek, Phys. Rev. B **94**, 224207 (2016).
[137] D. J. Luitz, N. Laflorencie, and F. Alet, Phys. Rev. B **93**, 060201 (2016).
[138] T. Enss, F. Andraschko, and J. Sirker, Phys. Rev. B **95**, 045121 (2017).

[139] B. Paredes, F. Verstraete, and J. I. Cirac, Phys. Rev. Lett. **95**, 140501 (2005).
[140] H. Kim and D. A. Huse, Phys. Rev. Lett. **111**, 127205 (2013).
[141] I. L. Aleiner, L. Faoro, and L. B. Ioffe, Ann. Phys. (N. Y). **375**, 378 (2016).
[142] A. I. Larkin and Y. N. Ovchinnikov, Jetp **28**, 1200 (1969).
[143] R. Fan, P. Zhang, H. Shen, and H. Zhai, Out-of-time-order correlation for many-body localization, (2016), arXiv:1608.01914.
[144] D. J. Luitz and Y. Bar Lev, Information propagation in isolated quantum systems, (2017), arXiv:1702.03929.
[145] T. Zhou and D. J. Luitz, Phys. Rev. B **95**, 094206 (2016), https://journals.aps.org/prb/abstract/10.1103/PhysRevB.95.094206.
[146] J. Hauschild, F. Heidrich-Meisner, and F. Pollmann, Phys. Rev. B **94**, 161109 (2016).
[147] V. K. Varma, A. Lerose, F. Pietracaprina, J. Goold, and A. Scardicchio, Energy diffusion in the ergodic phase of a many body localizable spin chain, (2015), arXiv:1511.09144.
[148] B. Li and J. Wang, Phys. Rev. Lett. **91**, 044301 (2003).
[149] R. Metzler, E. Barkai, and J. Klafter, Phys. Rev. Lett. **82**, 3563 (1999).
[150] R. Metzler and J. Klafter, Phys. Rep. **339**, 1 (2000).
[151] I. M. Sokolov and J. Klafter, Chaos **15**, 26103 (2005).
[152] D. Dhar and M. Barma, J. Stat. Phys. **22**, 259 (1980).
[153] R. G. Palmer, D. L. Stein, E. Abrahams, and P. W. Anderson, Phys. Rev. Lett. **53**, 958 (1984).
[154] M. Randeria, J. P. Sethna, and R. G. Palmer, Phys. Rev. Lett. **54**, 1321 (1985).
[155] D. Kutasov, A. Aharony, E. Domany, and W. Kinzel, Phys. Rev. Lett. **56**, 2229 (1986).
[156] P. Levy, Bull. la Société Mathématique Fr. **67**, 1 (1939).
[157] R. B. Griffiths, Phys. Rev. Lett. **23**, 17 (1969).
[158] T. Vojta, J. Phys. A. Math. Gen. **39**, R143 (2006).
[159] F. J. Dyson, Phys. Rev. **92**, 1331 (1953).
[160] A. Miller and E. Abrahams, Phys. Rev. **120**, 745 (1960).
[161] J. Kurkijärvi, Phys. Rev. B **8**, 922 (1973).
[162] J. Bernasconi, S. Alexander, and R. Orbach, Phys. Rev. Lett. **41**, 185 (1978).
[163] J. Bernasconi, W. R. Schneider, and W. Wyss, Zeitschrift für Phys. B Condens. Matterr Phys. B Condens. Matter Quanta **37**, 175 (1980).
[164] S. Alexander, Phys. Rev. B **23**, 2951 (1981).
[165] L. Zhang, B. Zhao, T. Devakul, and D. A. Huse, Phys. Rev. B **93**, 224201 (2016).
[166] R. Vosk and E. Altman, Phys. Rev. Lett. **110**, 067204 (2013).
[167] C. Dasgupta and S.-k. Ma, Phys. Rev. B **22**, 1305 (1980).
[168] D. S. Fisher, Phys. Rev. Lett. **69**, 534 (1992).
[169] D. S. Fisher, Phys. Rev. B **50**, 3799 (1994).
[170] D. S. Fisher, Phys. Rev. B **51**, 6411 (1995).
[171] K. Agarwal, E. A. Demler, and I. Martin, Phys. Rev. B **92**, 184203 (2015).
[172] A. Nauts and R. E. Wyatt, Phys. Rev. Lett. **51**, 2238 (1983).
[173] C. Moler and C. Van Loan, SIAM Review **45**, 3 (2003).
[174] W. E. Arnoldi, Quarterly of Applied Mathematics **9**, 17 (1951).
[175] M. Suzuki, Phys. Lett. A **146**, 319 (1990).
[176] A. T. Sornborger and E. D. Stewart, Phys. Rev. A **60**, 1956 (1999).
[177] M. Žnidarič, T. Prosen, and P. Prelovšek, Phys. Rev. B **77**, 064426 (2008).
[178] J. H. Bardarson, F. Pollmann, and J. E. Moore, Phys. Rev. Lett. **109**, 017202 (2012).
[179] M. Serbyn, Z. Papić, and D. A. Abanin, Phys. Rev. Lett. **110**, 260601 (2013).
[180] D.-L. Deng, X. Li, J. H. Pixley, Y.-L. Wu, and S. D. Sarma, Phys. Rev. B **95**, 024202 (2017).
[181] G. Vidal, Phys. Rev. Lett. **91**, 147902 (2003).
[182] G. Vidal, Phys. Rev. Lett. **93**, 040502 (2004).
[183] U. Schollwöck, Reviews of Modern Physics **77**, 259 (2005).
[184] G. Lindblad, Communications in Mathematical Physics **48**, 119 (1976).
[185] T. Prosen and M. Žnidarič, Journal of Statistical Mechanics: Theory and Experiment **2009**, P02035 (2009).
[186] M. Žnidarič, New Journal of Physics **12**, 043001 (2010).
[187] M. Ledoux, The concentration of measure phenomenon, Mathematical Surveys and Monographs, Vol. **89** (American Mathematical Society, Providence, RI, 2001).
[188] S. Popescu, A. J. Short, and A. Winter, Nat. Phys. **2**, 754 (2006).
[189] S. Goldstein, J. L. Lebowitz, R. Tumulka, and N. Zanghì, Phys. Rev. Lett. **96**, 050403 (2006).
[190] P. Reimann, Phys. Rev. Lett. **99**, 160404 (2007).
[191] C. Bartsch and J. Gemmer, Phys. Rev. Lett. **102**, 110403 (2009).
[192] D. Gelman and R. Kosloff, Chemical Physics Letters **381**, 129 (2003).
[193] S. Sugiura and A. Shimizu, Phys. Rev. Lett. **108**, 240401 (2012).
[194] S. Sugiura and A. Shimizu, Phys. Rev. Lett. **111**, 010401 (2013).
[195] T. A. Elsayed and B. V. Fine, Phys. Rev. Lett. **110**, 070404 (2013).
[196] R. Steinigeweg, A. Khodja, H. Niemeyer, C. Gogolin, and J. Gemmer, Phys. Rev. Lett. **112**, 130403 (2014).
[197] J. J. M. Cuppen, Numerische Mathematik **36**, 177 (1981).
[198] I. S. Dhillon, A New O (N(2)) Algorithm for the Symmetric Tridiagonal Eigenvalue/Eigenvector Problem, Ph.D. thesis, University of California at Berkeley, Berkeley, CA, USA (1998), uMI Order No. GAX98-03176.
[199] P. Amestoy, I. Duff, J. L'Excellent, and J. Koster, SIAM Journal on Matrix Analysis and Applications **23**, 15 (2001).

[200] P. R. Amestoy, A. Guermouche, J.-Y. L'Excellent, and S. Pralet, Parallel Computing Parallel Matrix Algorithms and Applications (PMAA'04), **32**, 136 (2006).
[201] X. S. Li, ACM Trans. Math. Softw. **31**, 302 (2005).
[202] X. Yu, D. Pekker, and B. K. Clark, Phys. Rev. Lett. **118**, 017201 (2017).
[203] M. Serbyn, A. A. Michailidis, D. A. Abanin, and Z. Papić, Phys. Rev. Lett. **117**, 160601 (2016).
[204] V. Khemani, F. Pollmann, and S. L. Sondhi, Phys. Rev. Lett. **116**, 247204 (2016).
[205] S. P. Lim and D. N. Sheng, Phys. Rev. B **94**, 045111 (2016).
[206] D. M. Kennes and C. Karrasch, Phys. Rev. B **93**, 245129 (2016).
[207] D. Pekker and B. K. Clark, Phys. Rev. B **95**, 035116 (2017).
[208] A. Chandran, J. Carrasquilla, I. H. Kim, D. A. Abanin, and G. Vidal, Physical Review B **92**, 024201 (2015).
[209] F. Pollmann, V. Khemani, J. I. Cirac, and S. L. Sondhi, Phys. Rev. B **94**, 041116 (2016).
[210] T. B. Wahl, A. Pal, and S. H. Simon, Efficient representation of fully many-body localized systems using tensor networks, (2016), arXiv:1609.01552.
[211] S. Inglis and L. Pollet, Phys. Rev. Lett. **117**, 120402 (2016).
[212] M. Serbyn, Z. Papić, and D. A. Abanin, Phys. Rev. Lett. **111**, 127201 (2013).
[213] D. A. Huse, R. Nandkishore, and V. Oganesyan, Phys. Rev. B **90**, 174202 (2014).
[214] A. Stan, N. E. Dahlen, and R. van Leeuwen, J. Chem. Phys. **130**, 224101 (2009).
[215] L. P. Kadanoff and G. Baym, Quantum Statistical Mechanics, edited by D. Pines (Westview Press, 1994) p. 224.
[216] V. Špička, B. Velický, and A. Kalvová, Phys. E Low-dimensional Syst. Nanostructures **29**, 154 (2005).
[217] V. Špička, B. Velický, and A. Kalvová, Phys. E Low-dimensional Syst. Nanostructures **29**, 196 (2005).
[218] S. Latini, E. Perfetto, A.-M. Uimonen, R. van Leeuwen, and G. Stefanucci, Phys. Rev. B **89**, 075306 (2014).
[219] S. Bera, G. De Tomasi, F. Weiner, and F. Evers, Density propagator for many-body localization: finite size effects, transient subdiffusion, (stretched-) exponentials, (2016), arXiv:1610.03085.
[220] T. Roscilde, P. Naldesi, and E. Ercolessi, SciPost Phys. **1**, 010 (2016).
[221] H. P. Lüschen, P. Bordia, S. Scherg, F. Alet, E. Altman, U. Schneider, and I. Bloch, Evidence for Griffiths-Type Dynamics near the Many-Body Localization Transition in Quasi-Periodic Systems, (2016), arXiv:1612.07173.
[222] Y. Bar Lev, D. M. Kennes, C. Klöckner, D. R. Reichman, and C. Karrasch, Transport in quasiperiodic interacting systems: from superdiffusion to subdiffusion, (2017), arXiv:1702.04349.
[223] F. Huveneers, Ann. Phys. (Berlin) **529**, 1600384 (2017).
[224] K. H. Fischer and J. A. Hertz, Spin Glasses, Cambridge Studies in Magnetism (Cambridge University Press, 1993).
[225] M. Schiulaz and M. Müller, in AIP Conf. Proc. (2014) pp. 11–23.
[226] N. Y. Yao, C. R. Laumann, J. I. Cirac, M. D. Lukin, and J. E. Moore, Phys. Rev. Lett. **117**, 240601 (2016).
[227] M. Schiulaz, A. Silva, and M. Müller, Phys. Rev. B **91**, 184202 (2015).
[228] J. M. Hickey, S. Genway, and J. P. Garrahan, J. Stat. Mech. Theory Exp. **2016**, 054047 (2016).
[229] W. De Roeck and F. Huveneers, Commun. Math. Phys. **332**, 1017 (2014).
[230] W. De Roeck and F. Huveneers, Phys. Rev. B **90**, 165137 (2014).
[231] Z. Papić, E. M. Stoudenmire, and D. A. Abanin, Ann. Phys. (N. Y). **362**, 714 (2015).
[232] W. D. Roeck and F. Huveneers, in From Part. Syst. to Partial Differ. Equations II, Springer Proceedings in Mathematics & Statistics, Vol. **129**, edited by P. Gonçalves and A. J. Soares (Springer International Publishing, Cham, 2015) pp. 173–192.
[233] M. van Horssen, E. Levi, and J. P. Garrahan, Phys. Rev. B **92**, 100305 (2015).
[234] J. R. Garrison, R. V. Mishmash, and M. P. A. Fisher, Phys. Rev. B **95**, 054204 (2016), https://journals.aps.org/prb/abstract/10.1103/PhysRevB.95.054204.
[235] A. E. Antipov, Y. Javanmard, P. Ribeiro, and S. Kirchner, Phys. Rev. Lett. **117**, 146601 (2016).
[236] J.-P. Bouchaud, L. Cugliandolo, J. Kurchan, and M. Mézard, Phys. A Stat. Mech. its Appl. **226**, 243 (1996).
[237] E. B. Bogomolny, U. Gerland, and C. Schmit, Phys. Rev. E **59**, R1315 (1999).